Part 2

Cryo-SEM

Scanning Electron Microscope (SEM) --*Surface imaging*

- Highly viscous systems
- Fine details in large objects
- HR Cryo-SEM (FEG, detectors)

The Technion's Zeiss Ultra Plus High-Resolution Scanning Electron Microscope (HR-SEM)

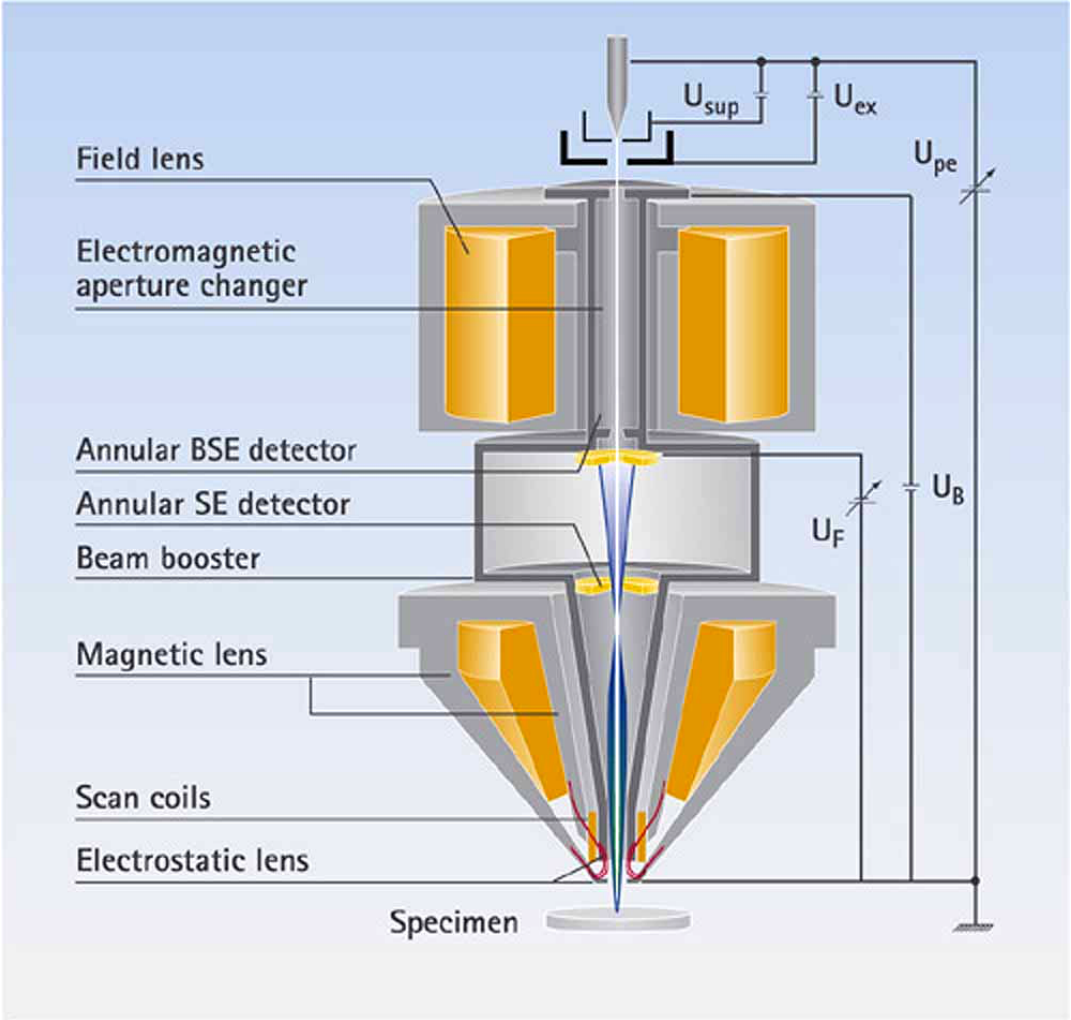

The Gemini System, e.g., in the Zeiss Ultra *Plus*

Cryo-SEM Specimen preparation

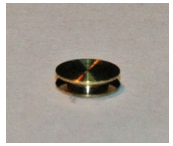

Sandwich

Gold planchettes
(R=4.6mm)

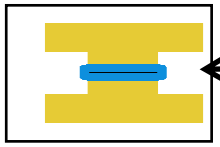

Sample
volume=3µl

Schematic
view of
sandwich

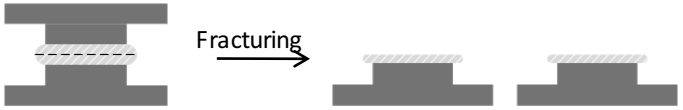

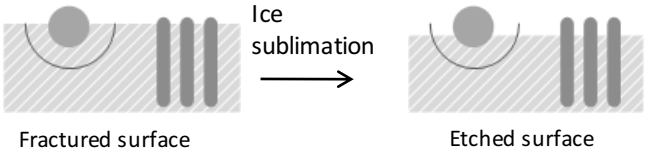

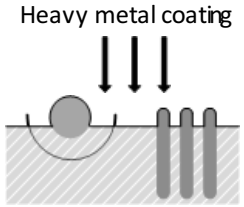

CEVS for cryo-SEM- system components

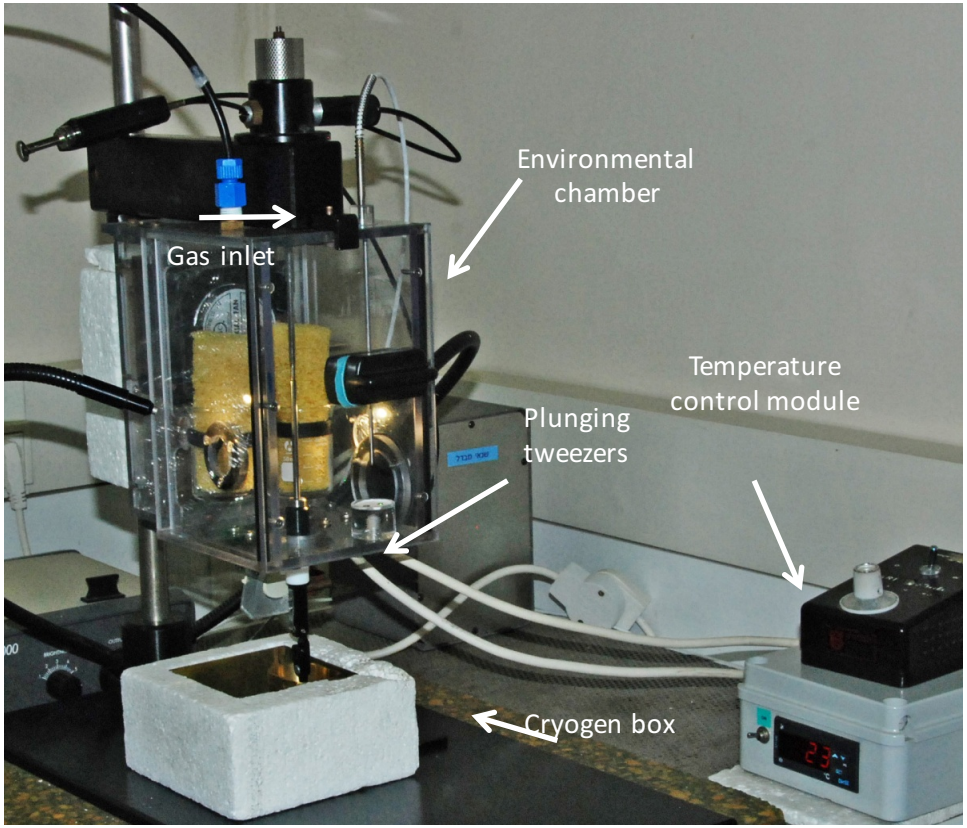

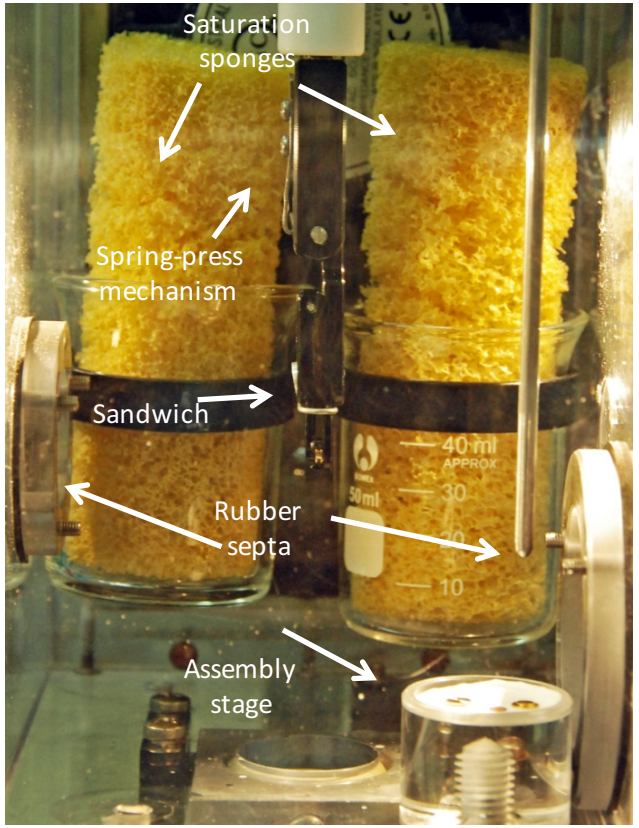

Issman, L. and Talmon, Y., J. Microscopy (2012)

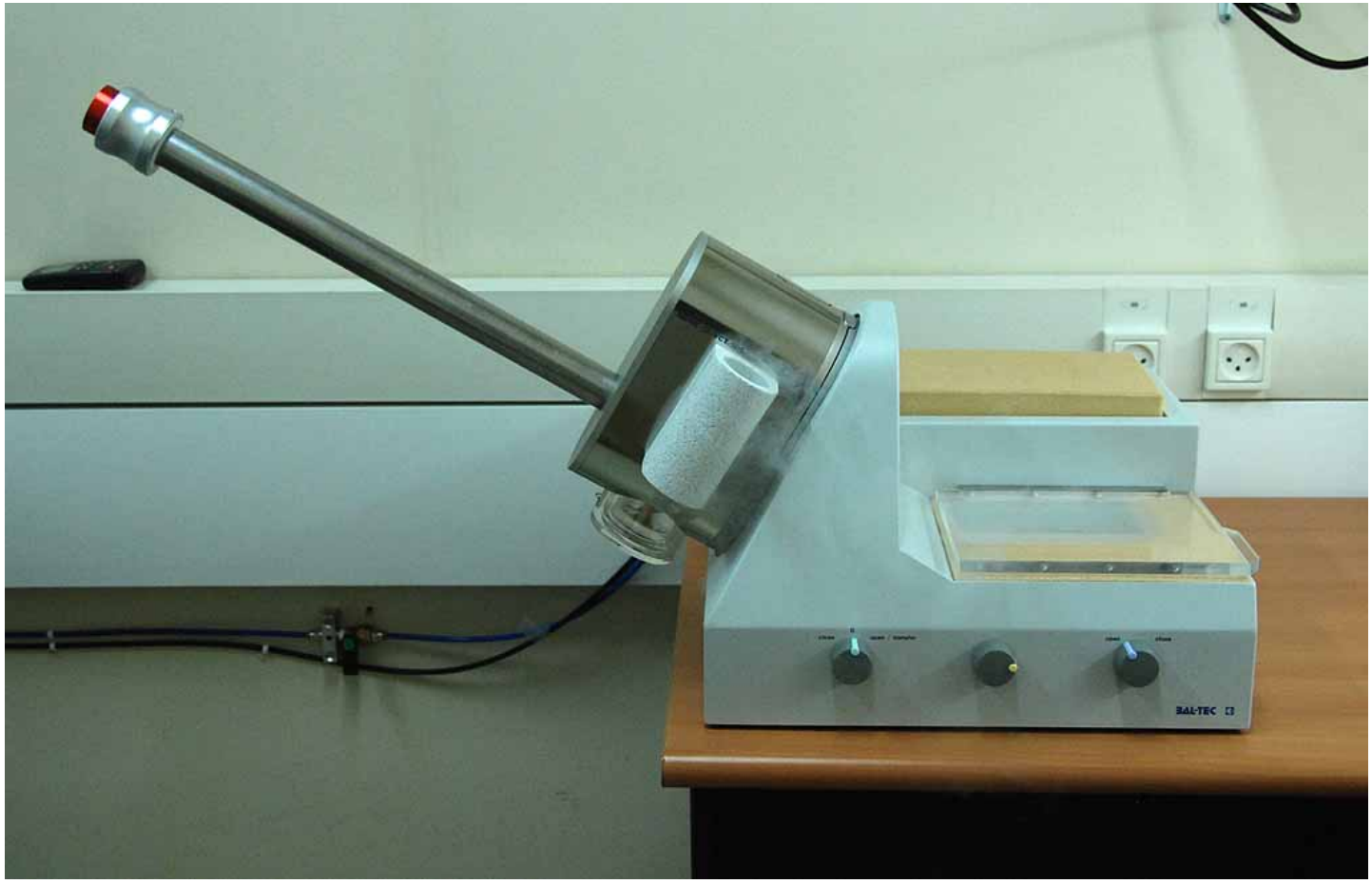

Cryo-SEM: “specimen-table” loading

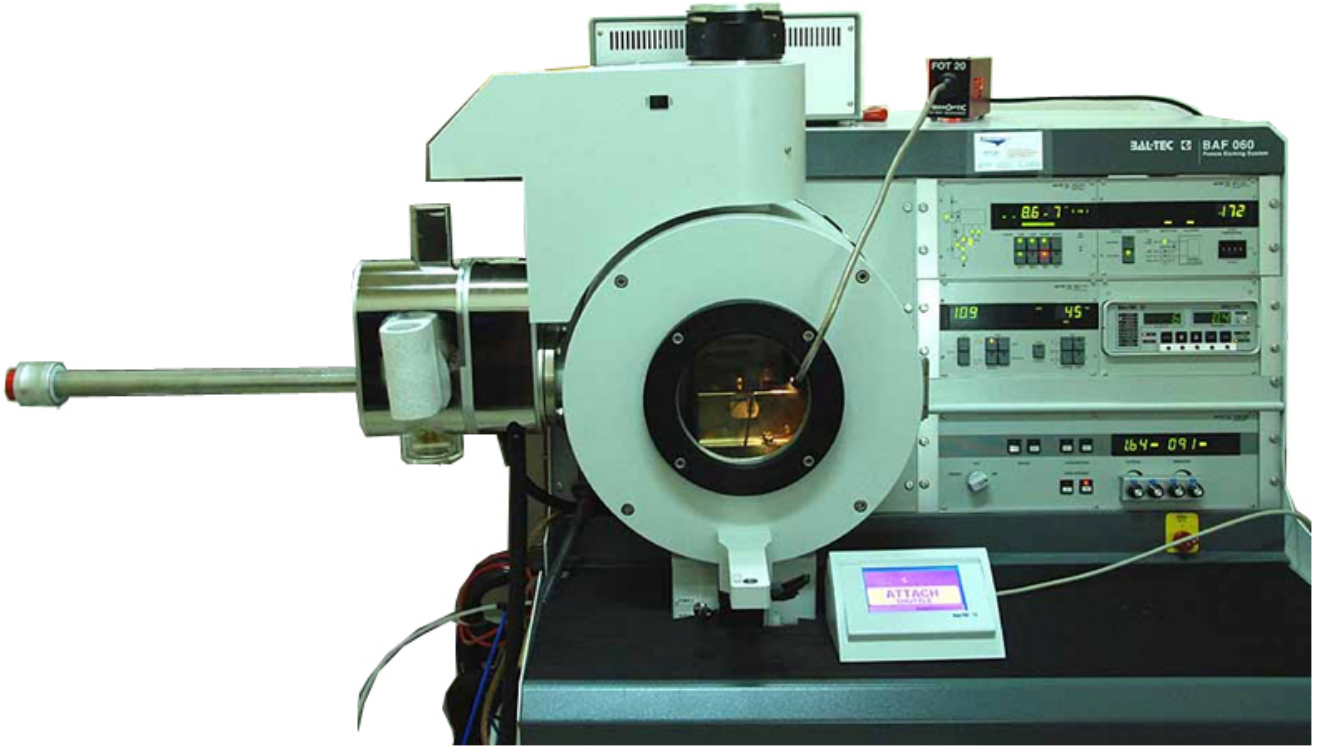

The BAF 060: fracture and coat for cryo-SEM, or prepare freeze-fracture replicas (FFR)

Cryo-SEM: Shuttle attached to the Zeiss Ultra Plus

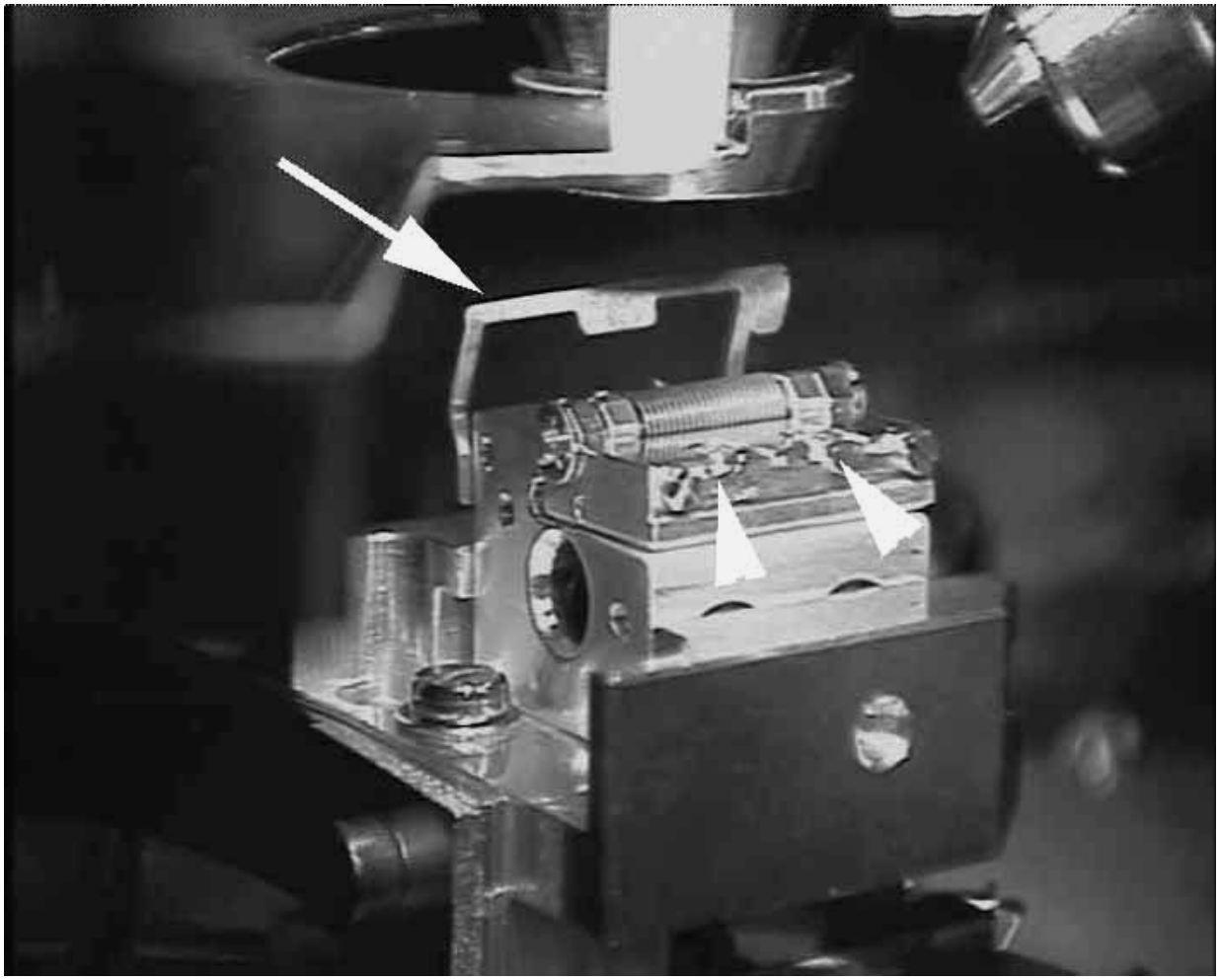

Cryo-SEM: Specimen-table on the SEM cryo-stage

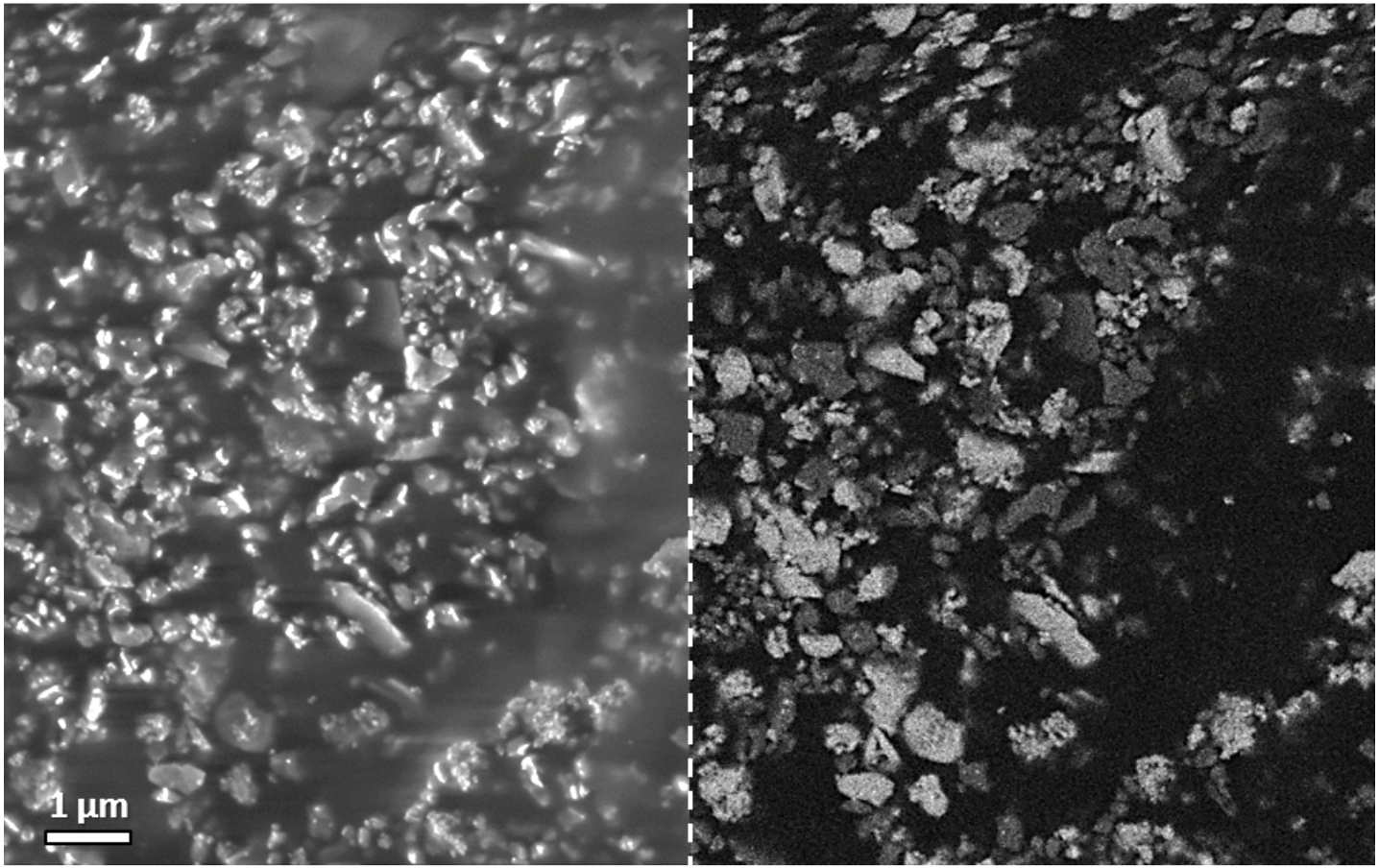

Al_2O_3 & Y_2O_3 in 100% ethanol; SE2 (left); InLens (right); Liron Issman

Holder for Surface Top-View

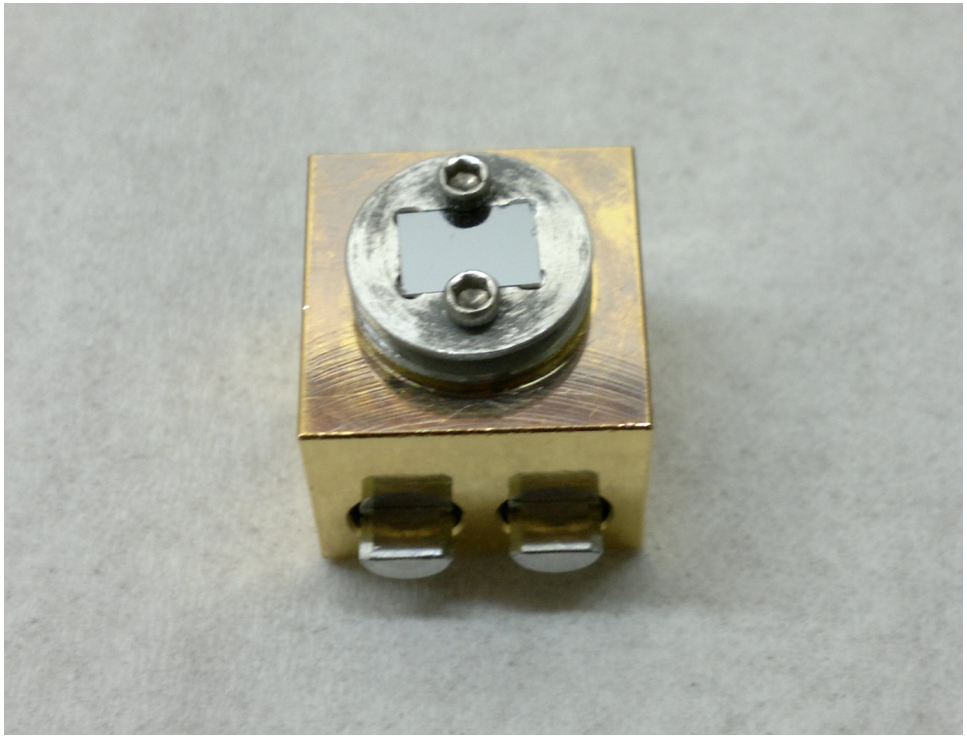

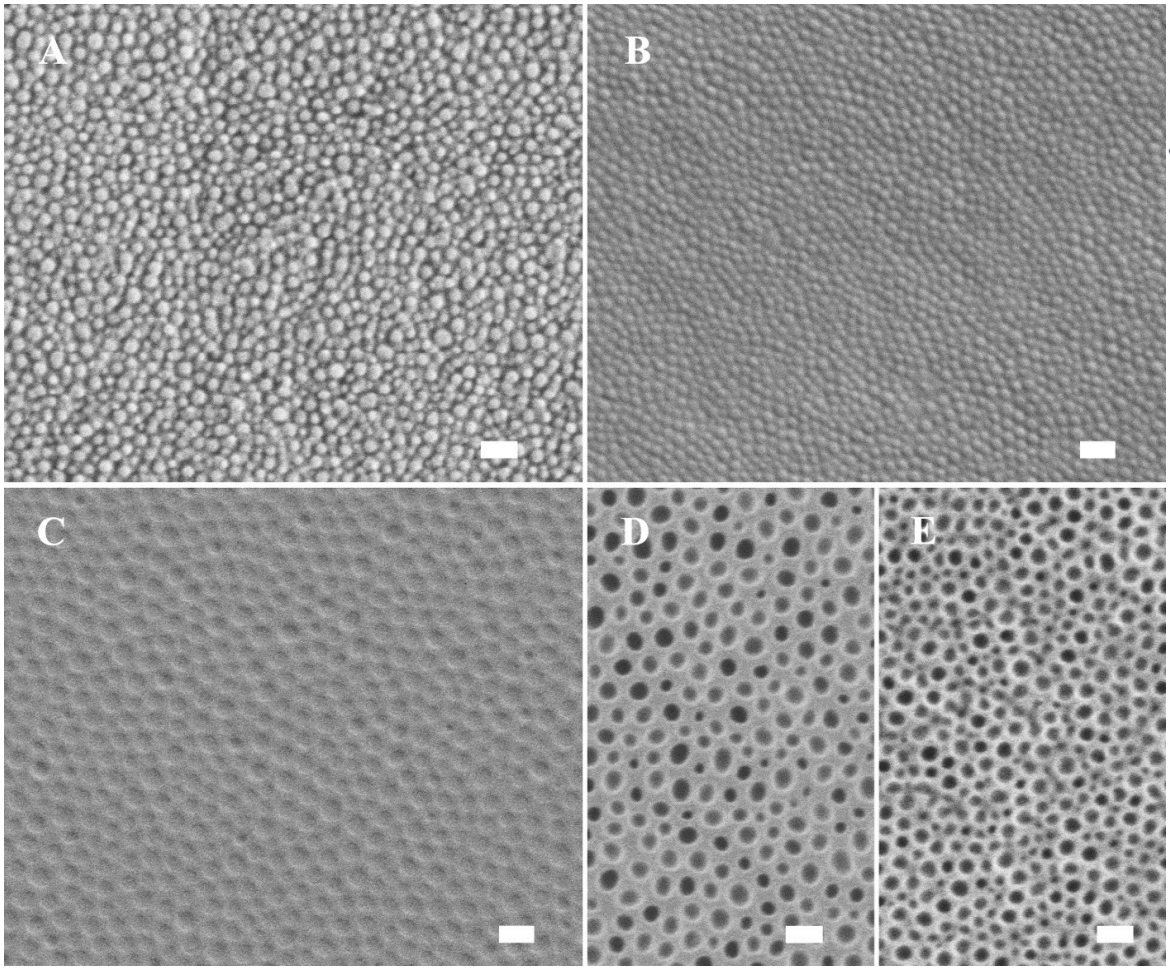

Liat Ronen et al., Macromolecules (2012)

Cryo (A to D) and RT (E) HR-SEM of membranes prepared from 20% PS_{73}-*b*-$P4VP_{27}$, 310 kg/mol in 70% / 30% DMF/THF: A. 11 s evaporation time; B. 18 s evaporation time; C. 25 s evaporation time; D. 40 s evaporation time; E. dried membrane. Bars are 200 nm.

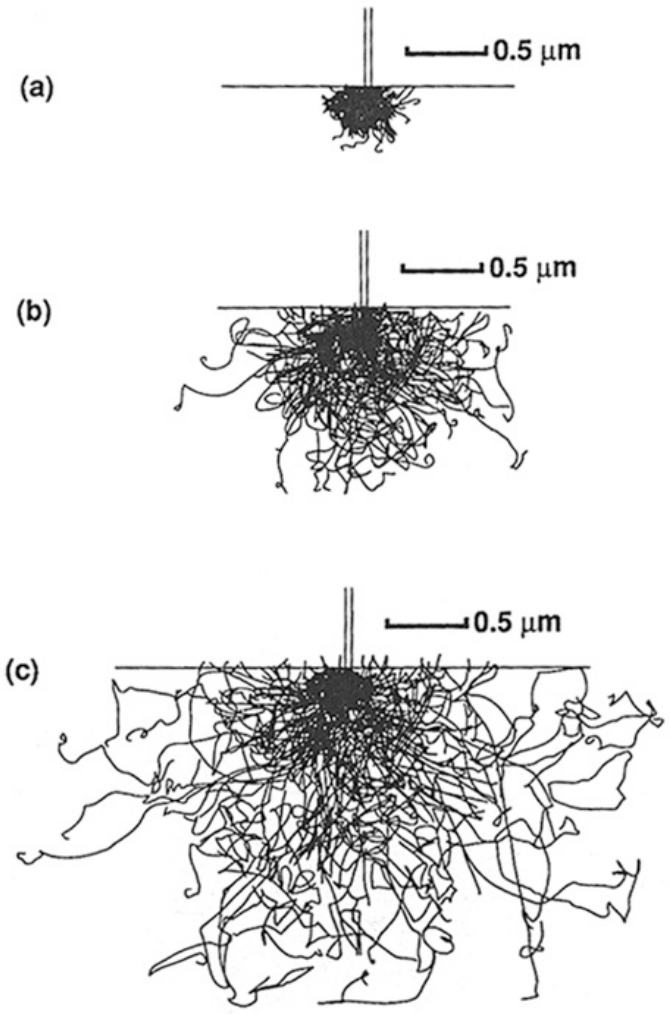

Figure 3.8. Monte Carlo electron-trajectory simulations of the interaction volume in iron as a function of beam energy: (a) 10 keV, (b) 20 keV, (c) 30 keV.

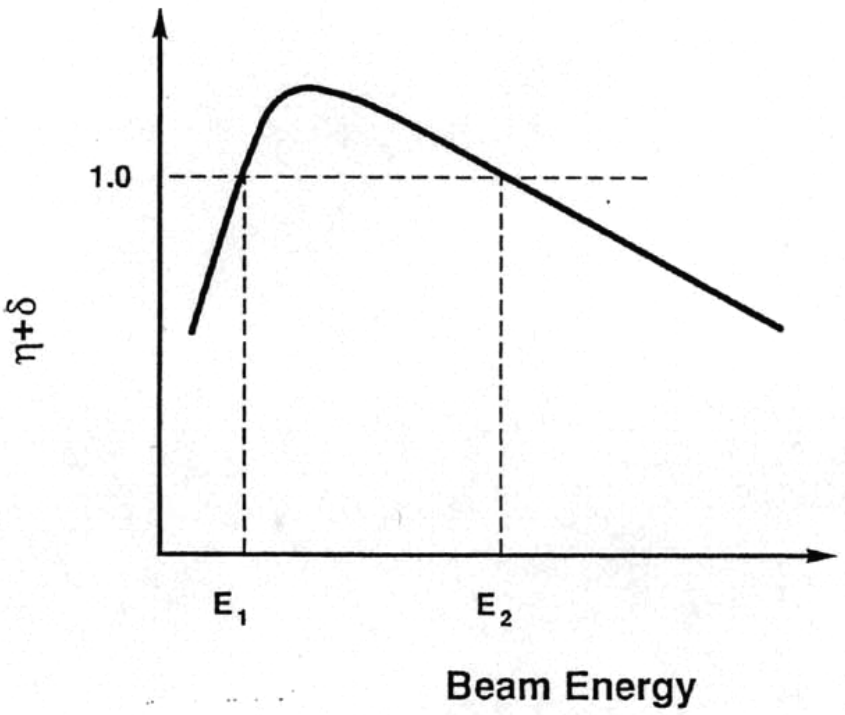

Figure 3.18. Schematic illustration of the total emitted electron coefficient $(\eta + \delta)$ as a function of beam energy.

Echlin, Patrick, et al. *Advanced scanning electron microscopy and X-ray microanalysis*. Springer Science & Business Media, 2013.

Table 3.6. Upper Crossover Energy for Various Materials (Normal Beam Incidence)

Material	E_2(keV)	Reference
Kapton	0.4	Joy (unpublished)
Electron resist	0.55–0.70	Joy(1987)
Nylon	1.18	Joy (unpublished)
5% PB7/nylon	1.40	Krause *et al.* (1987)
Acetal	1.65	Vaz (1986)
Polyvinyl chloride	1.65	Vaz (1986)
Teflon	1.82	Vaz and Krause (1986)
Glass passivation	2.0	Joy (1987)
GaAs	2.6	Joy (1987)
Quartz	3.0	Joy (1987)
Alumina	4.2	Joy (unpublished)

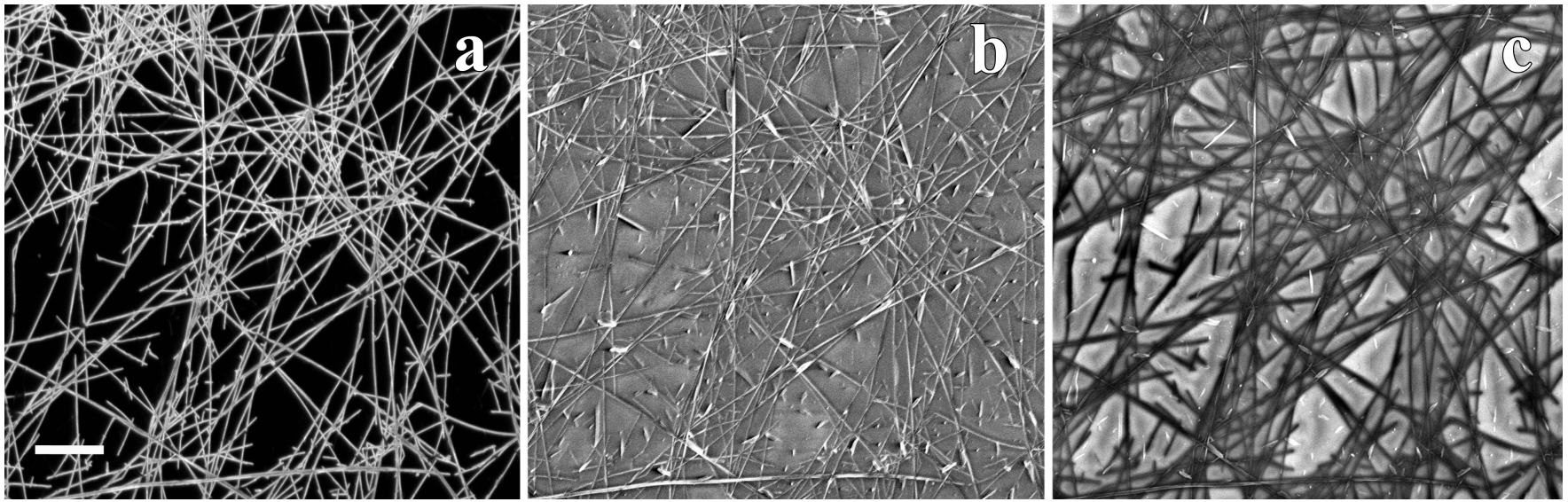

Thin CNT film on a glass slide; partial coverage

Zeiss Ultra Plus, “InLens” secondary electron detector, WD = 3.5 mm

(a) 0.5 kV, (b) 2 kV, (c) 3 kV

Scale bar = 2 µm

Dr. Olga Kleinerman

Cryo-SEM of a 5000 ppm HiPco CNTs in CSA

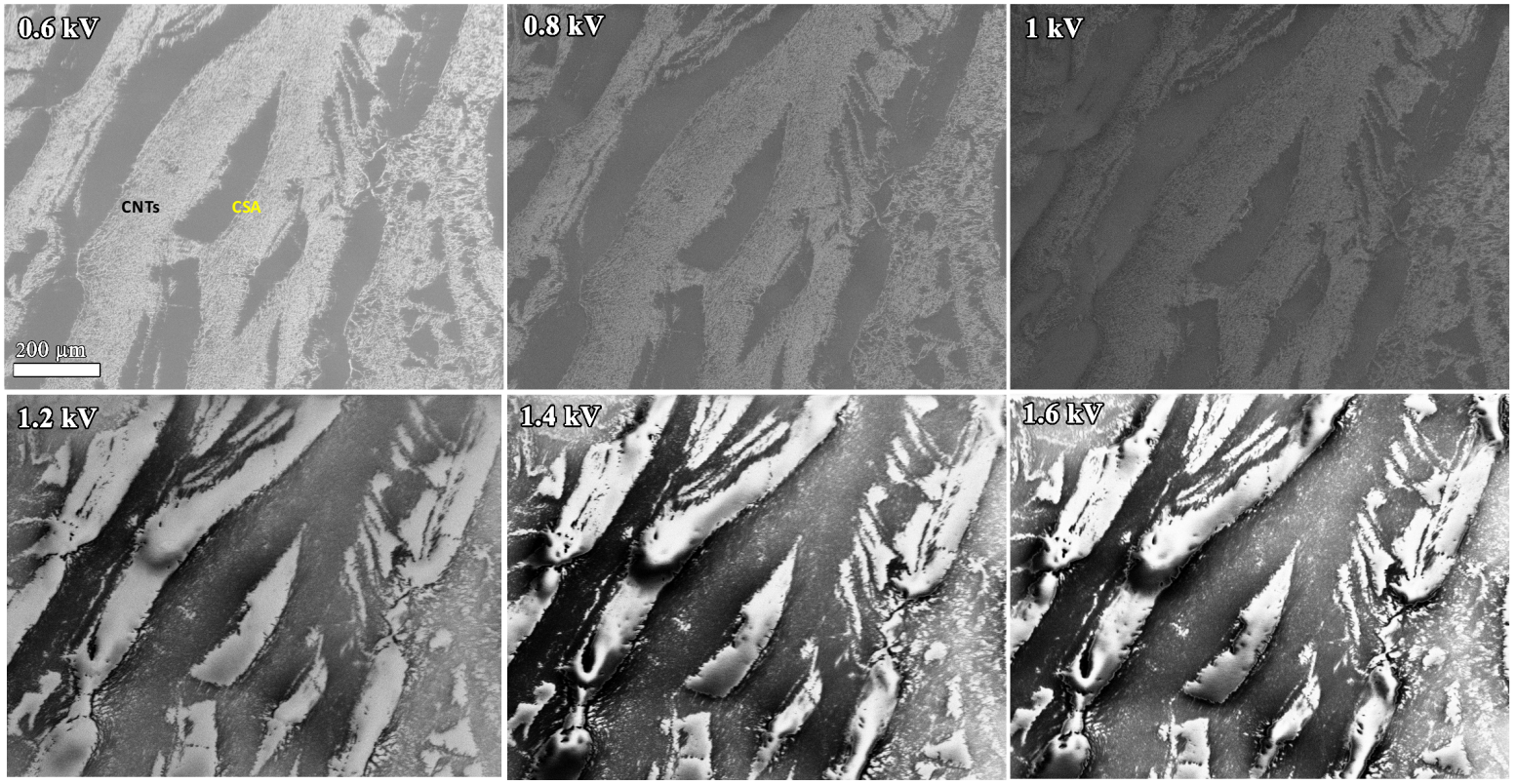

Zeiss Ultra Plus, InLens detector

Lucy Liberman

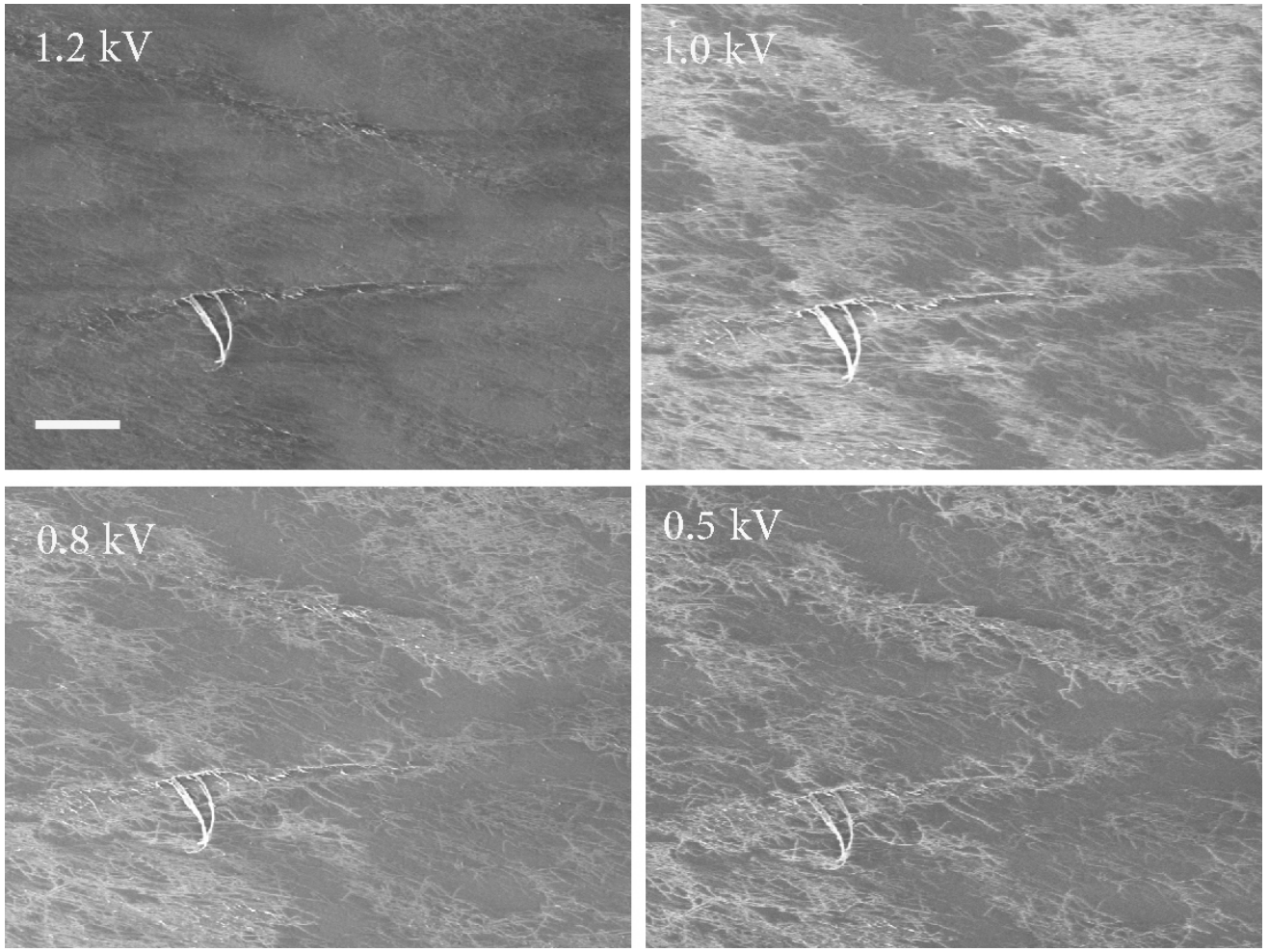

CNTs in water, InLens detector. Bar = 2 µm Lucy Liberman

Paraffin wax on glass

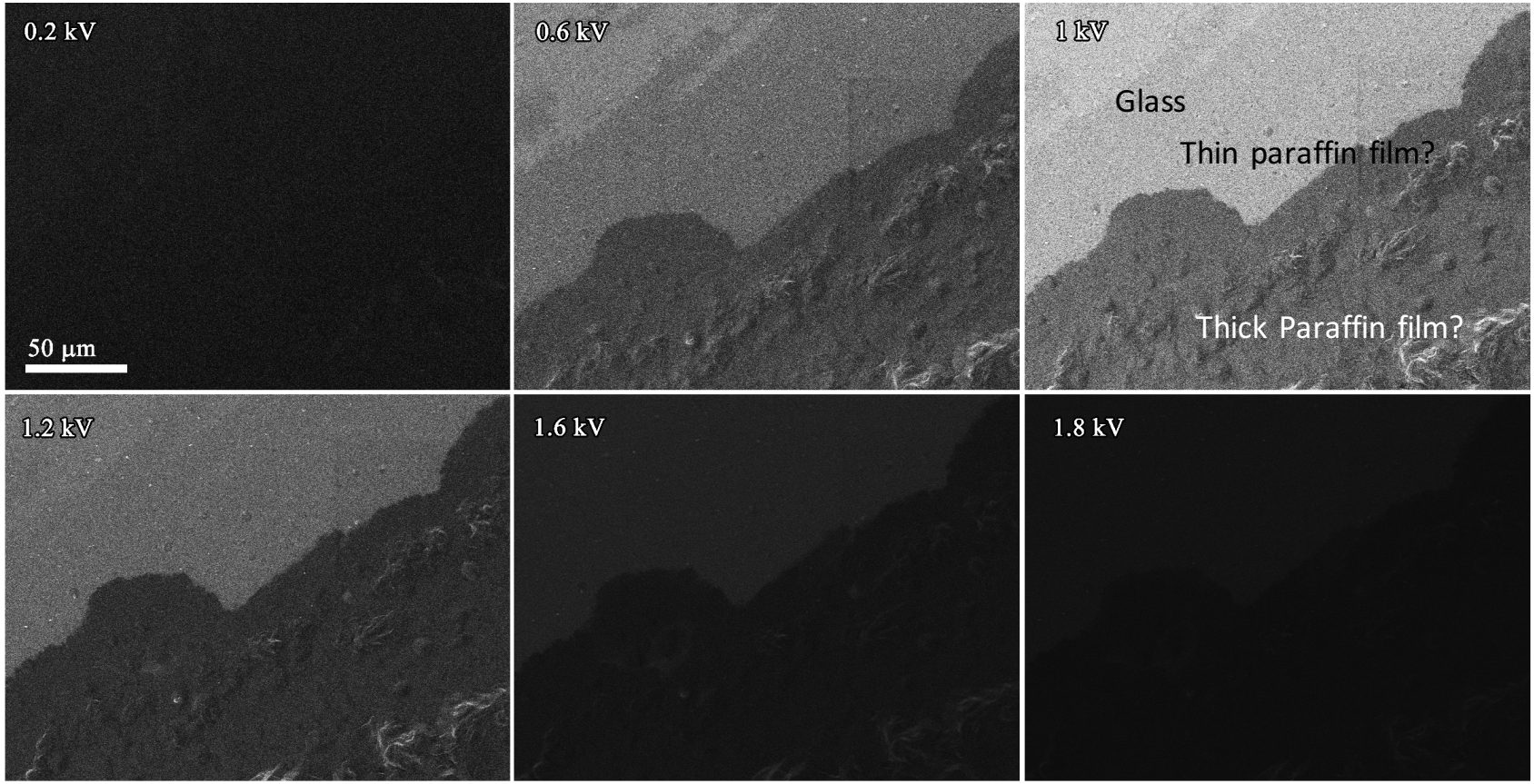

Zeiss Ultra Plus, SE2 detector

FEI Helios FEG SEM/(FIB)

Ned Thomas (Rice U.)

Paraffin wax (left) over silicon wafer

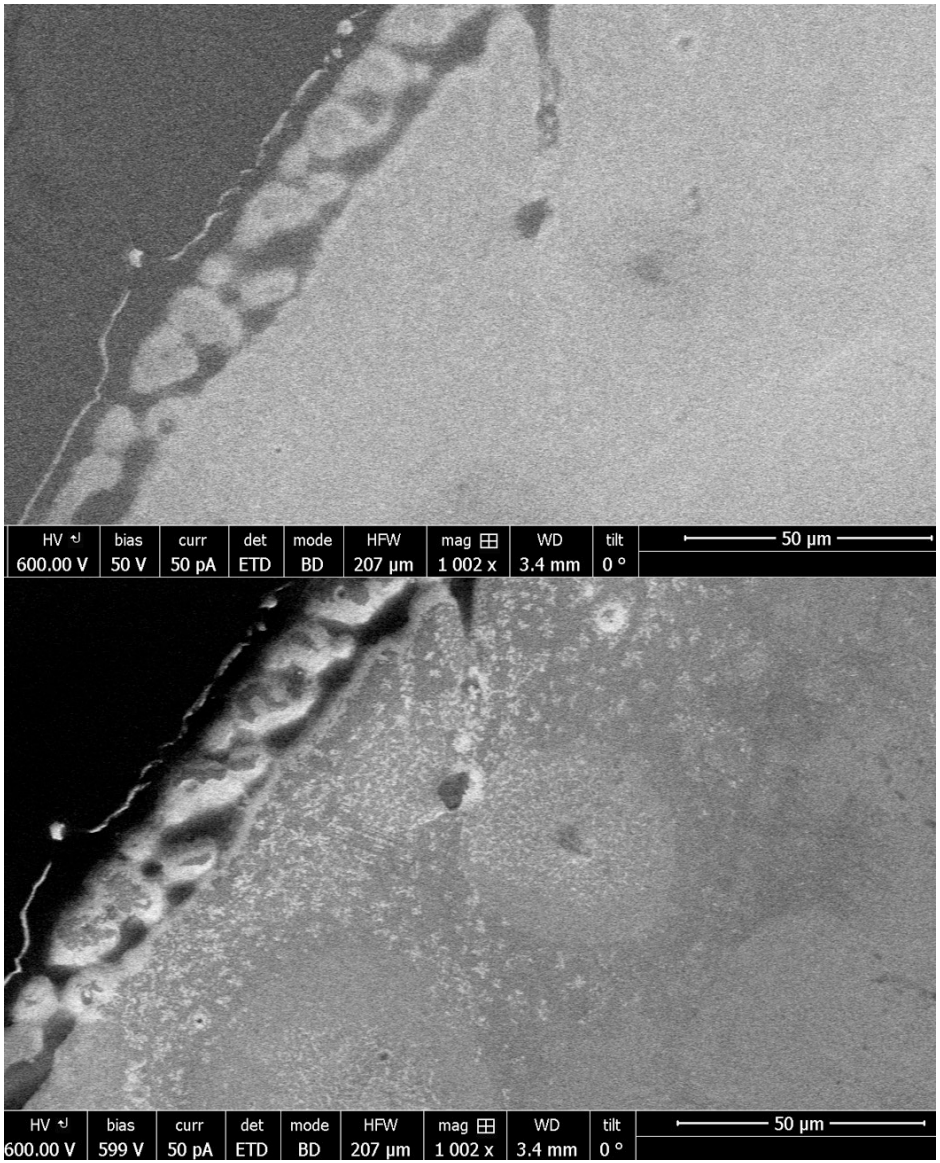

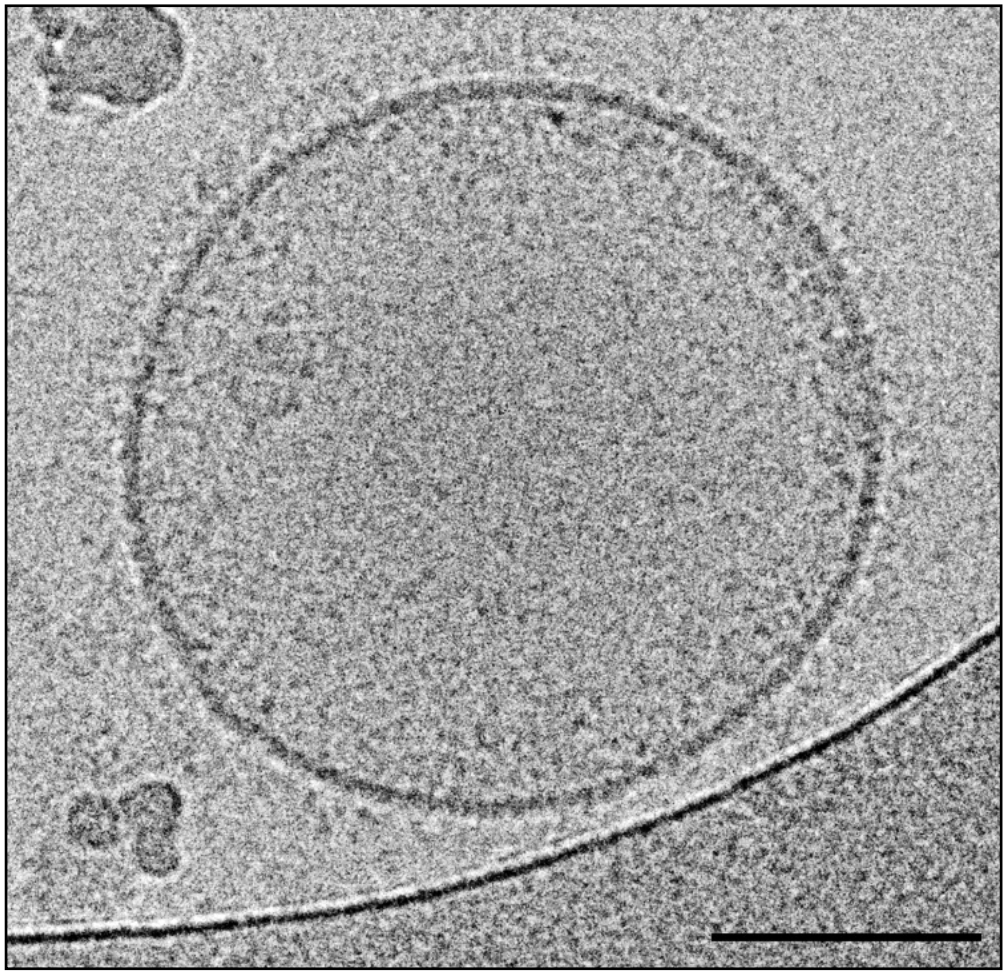

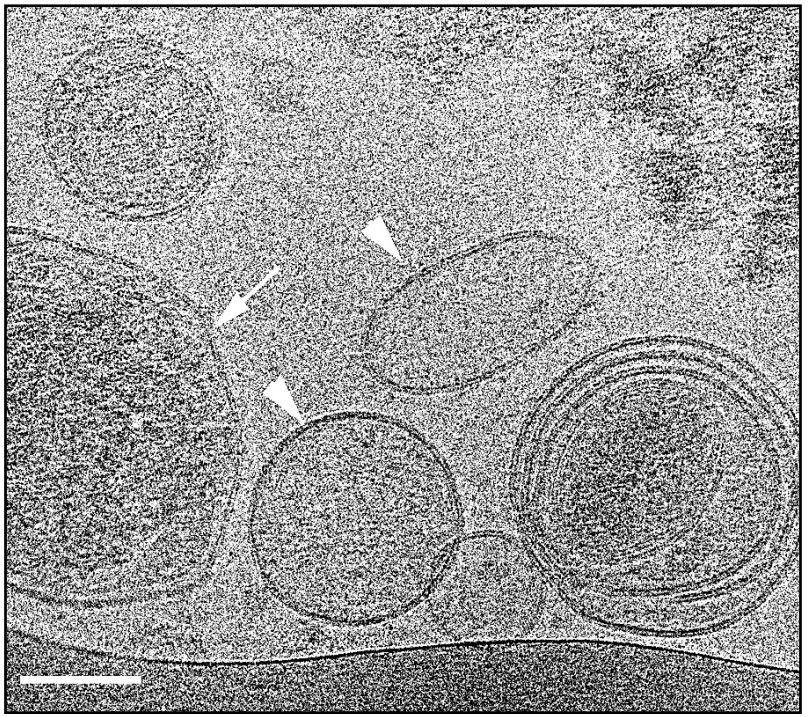

Cryo-TEM micrographs of extracellular vesicles isolated from THP1 cells after 4 hr LPS stimulation.

Idan Biran

Bars = 100 nm

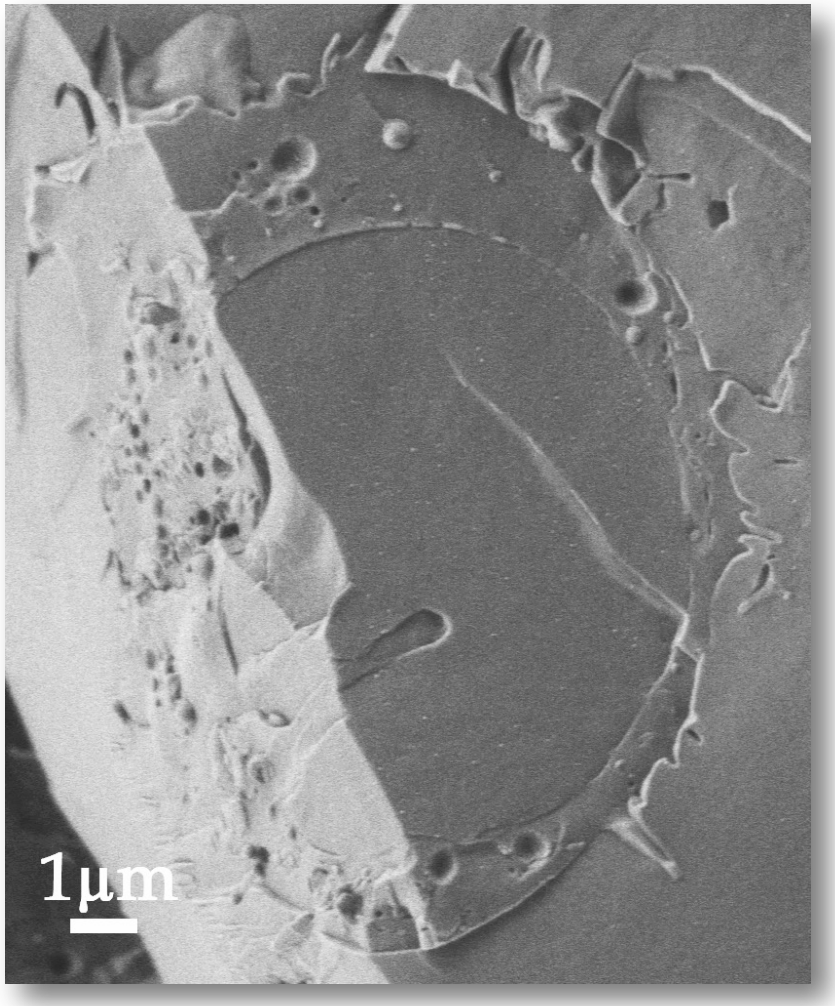

Koifman et al., J. Structural Biol. (2017)

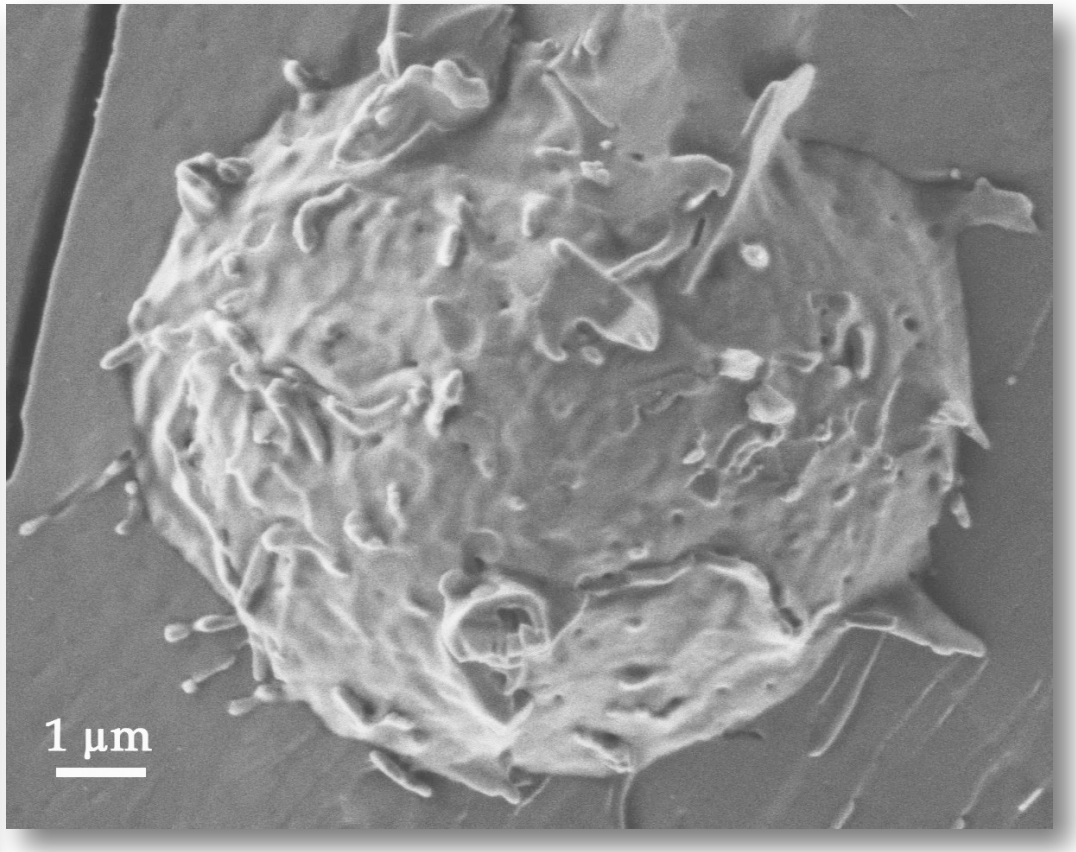

Cryo-SEM of monocytes after
48 hours starvation

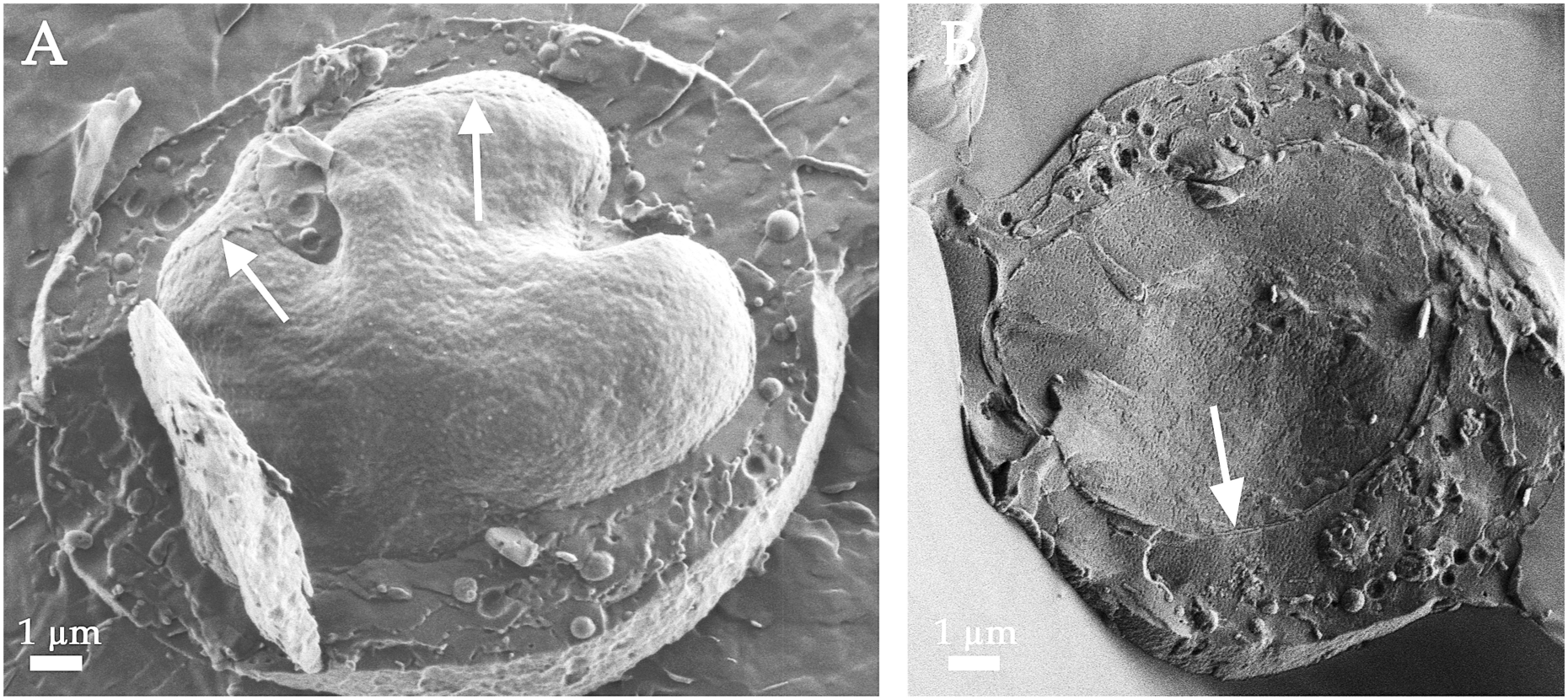

THP1 cells non-stimulated (A, B); specimen prepared by HPF (A) and by the drop method (B); no significant blebbing or microvesicles are evident. The partially removed nuclear membrane is visible (white arrows, A) and its cross-section (white arrow, B).

Koifman et al., J. Structural Biol. (2017)

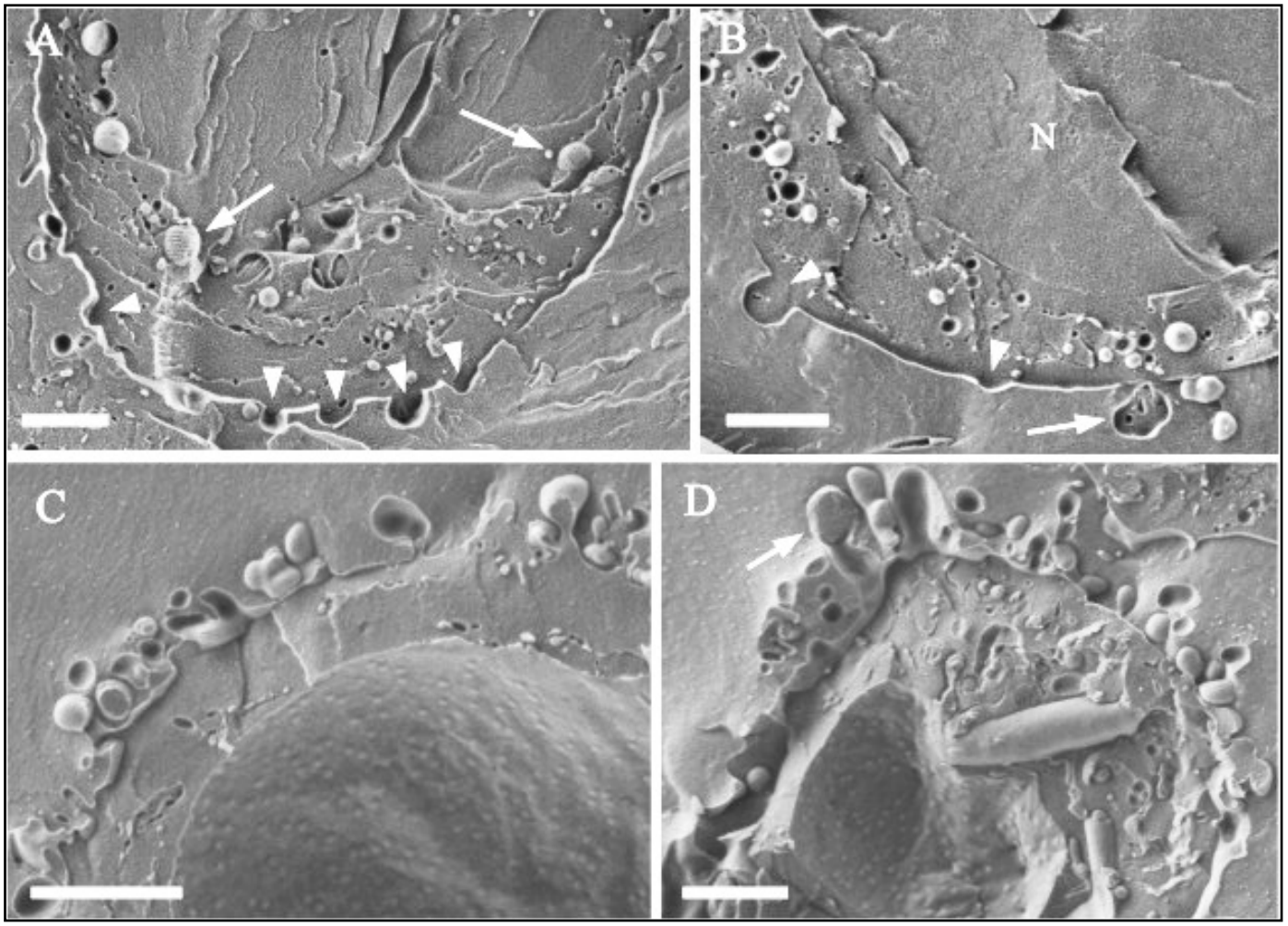

Cryo SEM of a fractured THP1 monocyte after 4 hr LPS (lipopolysaccharide) stimulation; Bars = 2 µm

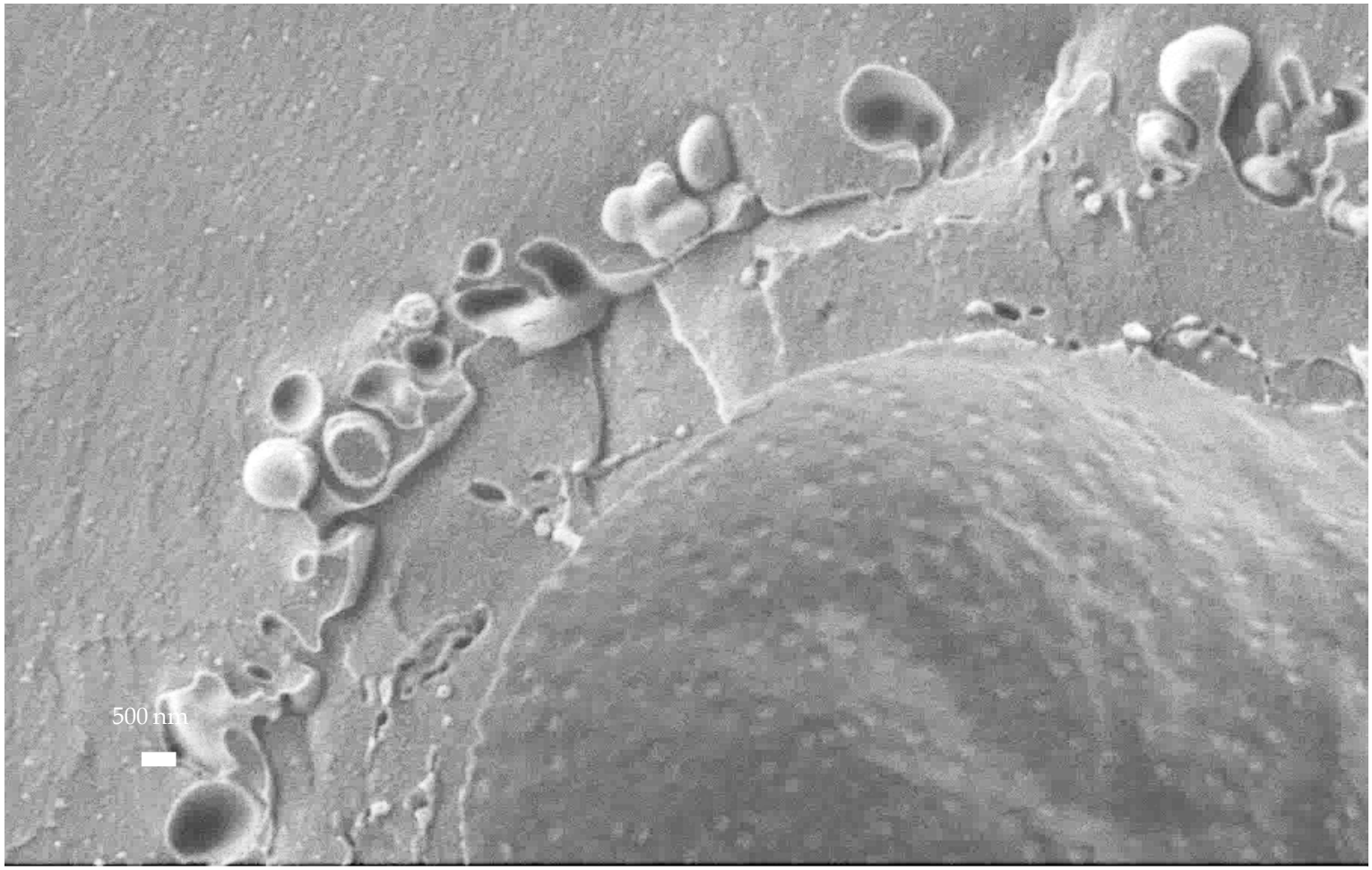

Cryo-SEM of a fractured THP1 monocyte after 4 hr LPS stimulation

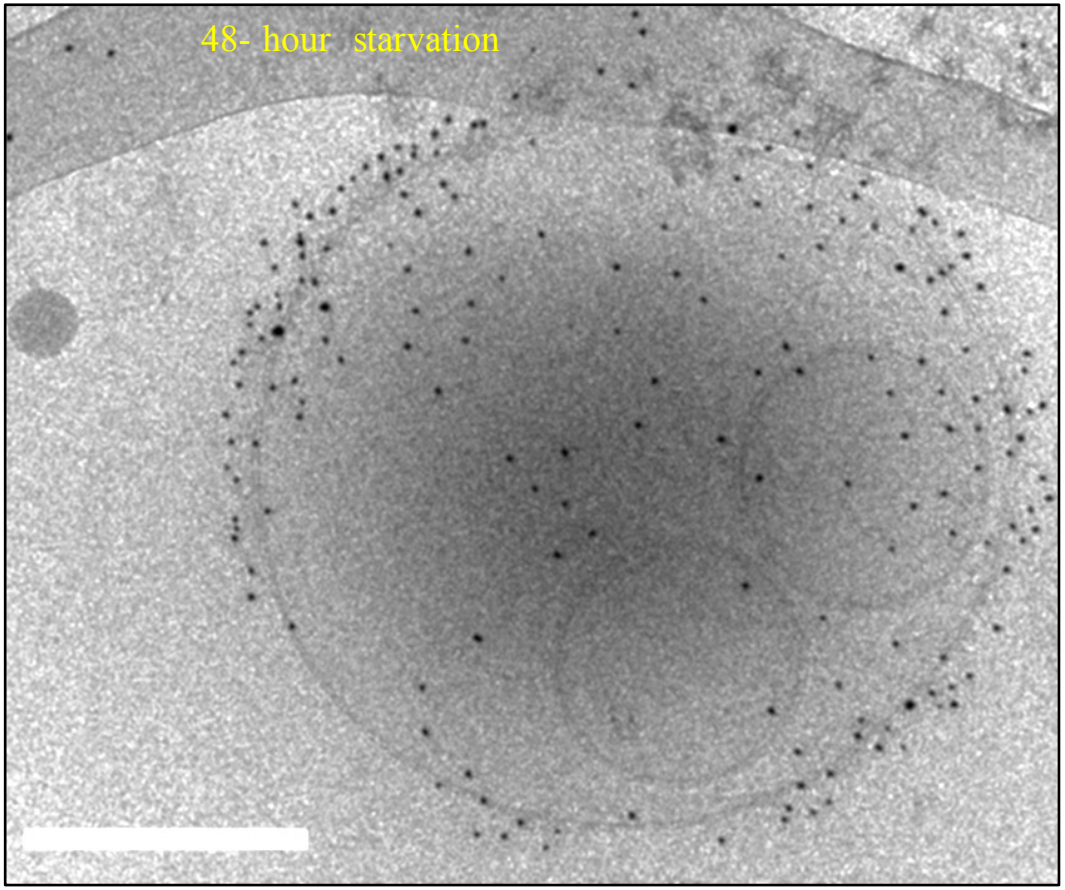

In-the-liquid-phase immunogold-labeled EV from THP1 Cell

Bar = 100 nm; Idan Biran

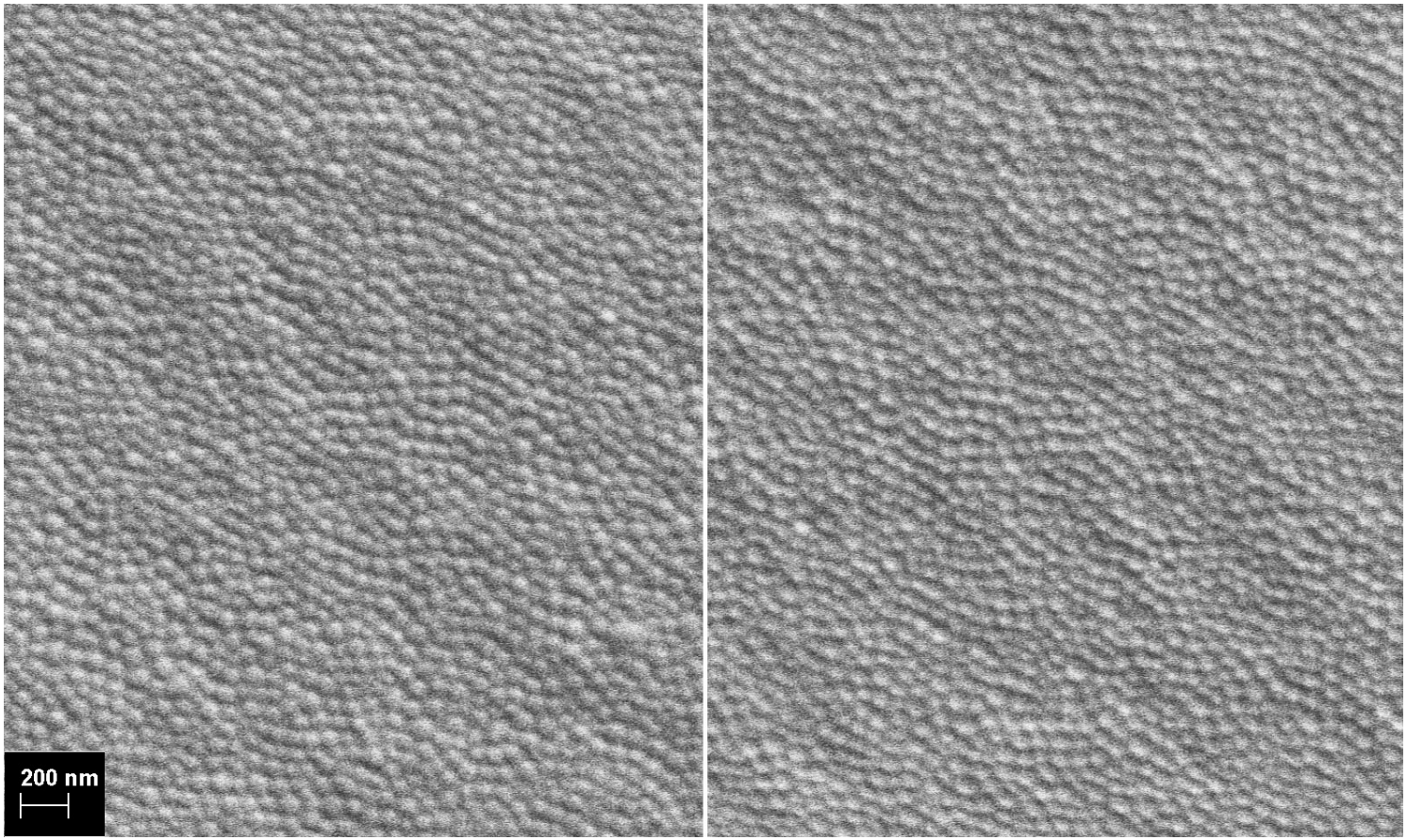

Cryo-SEM of cast block-copolymer film. Left & right are the same area rotated 180°

The fortess of Allepo (Hallab). Left & right are same picture, rotated 180˚

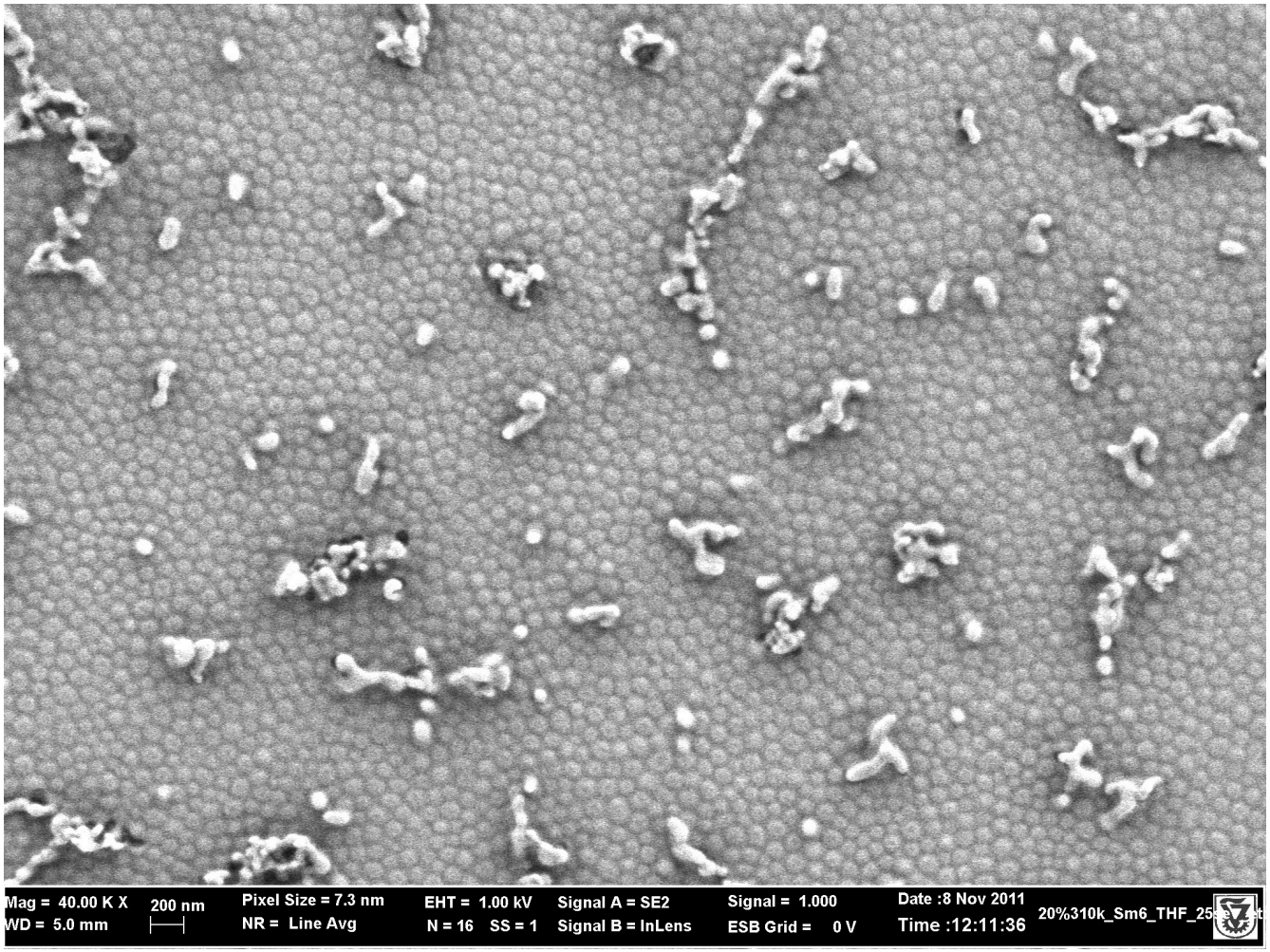

Surface contamination helps telling holes from bumps

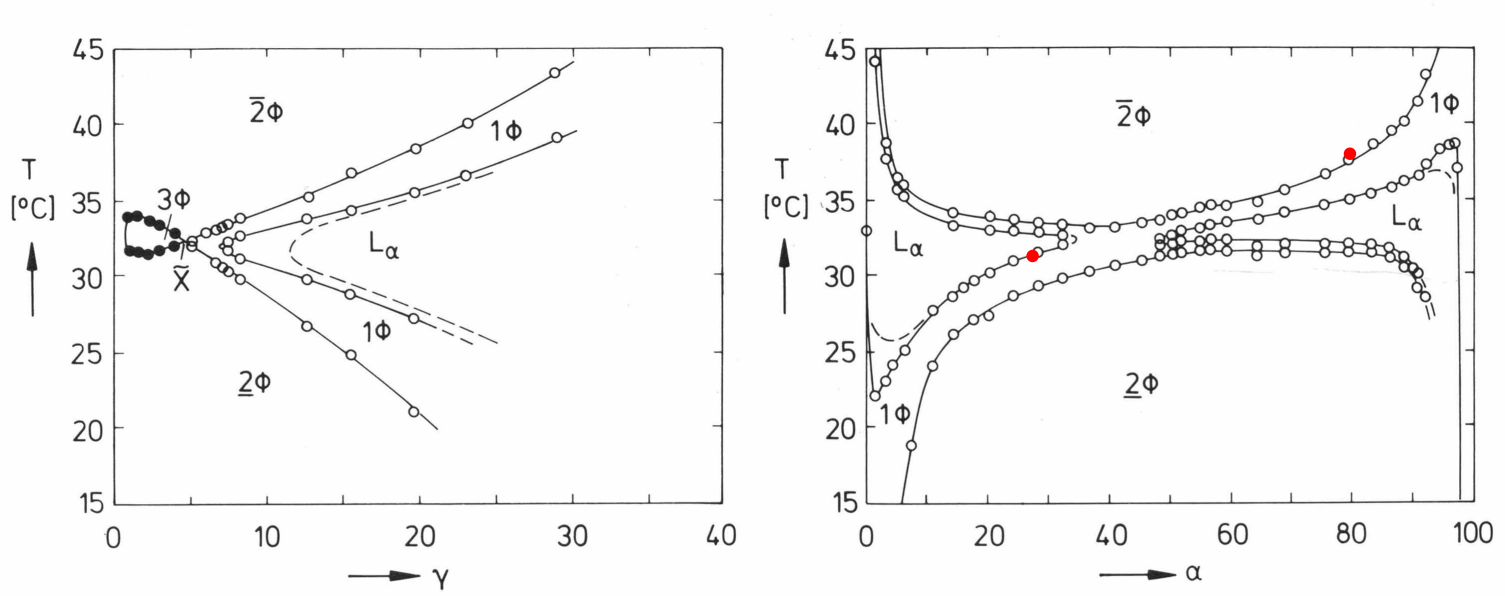

FIG. 3. Left: Vertical section through the phase prism of the system H_2O–*n*-octane–$C_{12}E_5$ at α = 40 wt% with lower ($\underline{2}\Phi$), upper ($\bar{2}\Phi$) two-phase body and three-phase (3Φ) body between. Also shown is the region of the lamellar mesophase (L_α). Right: Vertical section through the same prism at γ = 7 wt%, showing the isotropic homogeneous channel from the H_2O-rich to the oil-rich side.

Kahlweit, R. Strey, J. Phys. Chem. **90** (1986) 5239

$\alpha = 80$
36 ˚C

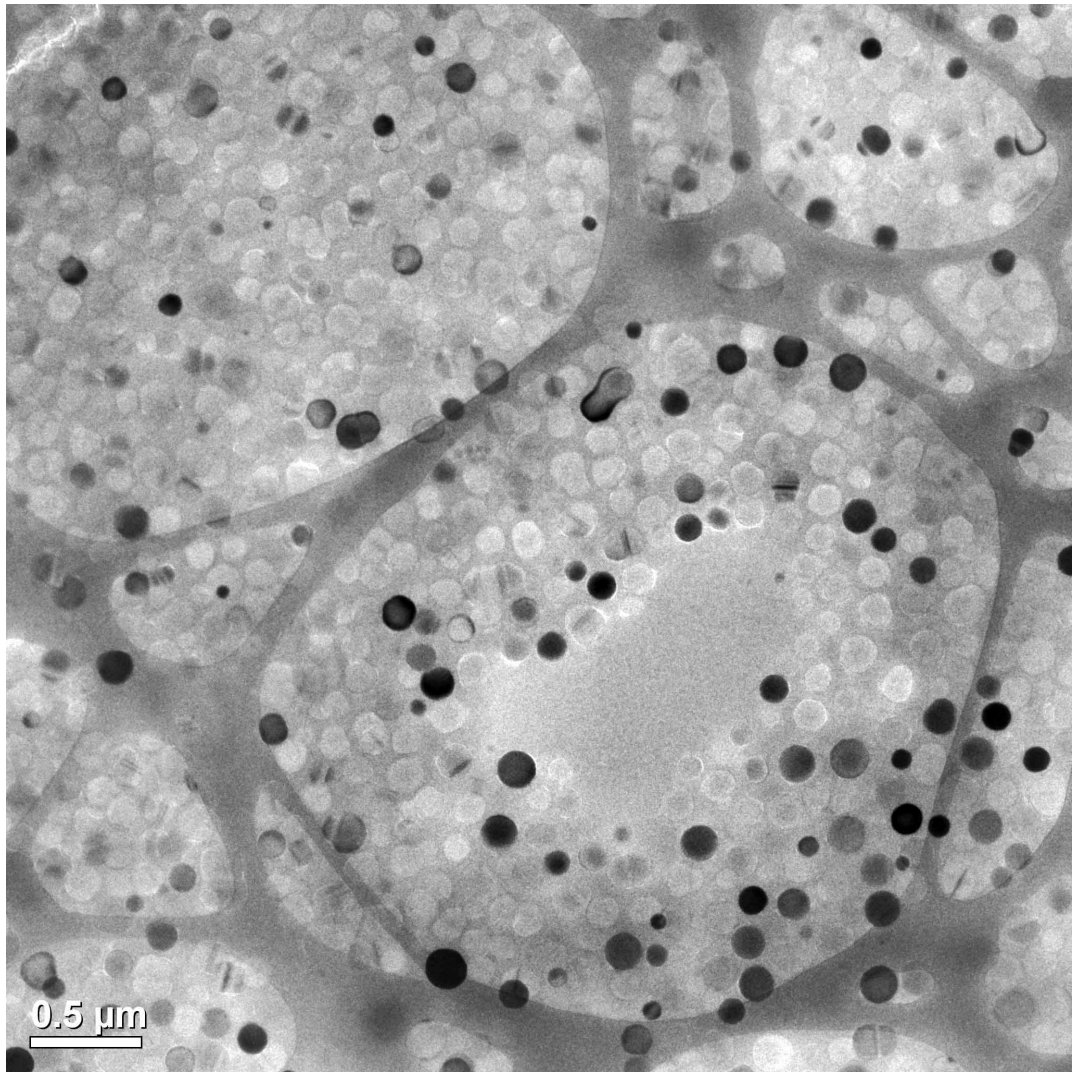

$\alpha = 70$
30 ˚C

Liron Issman

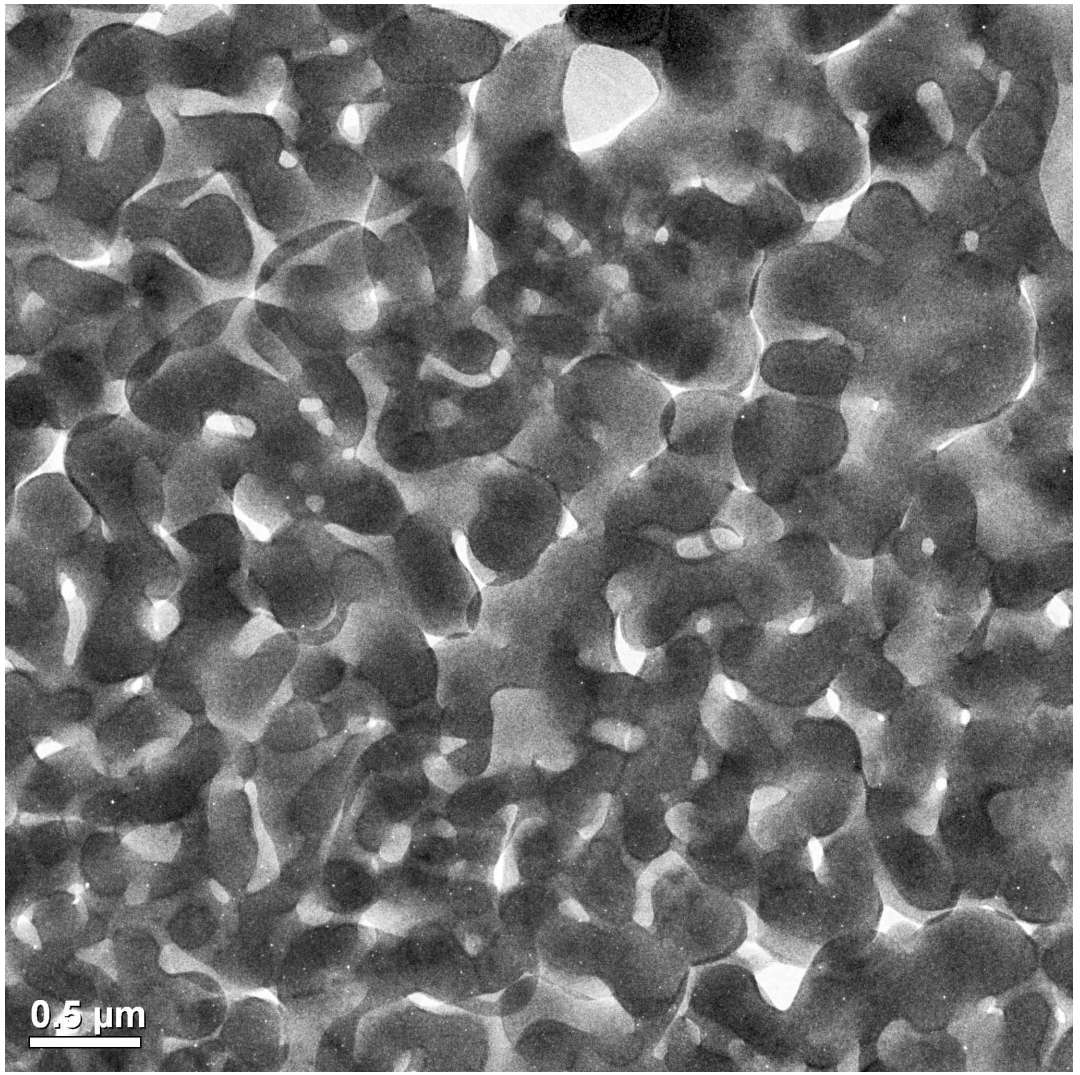

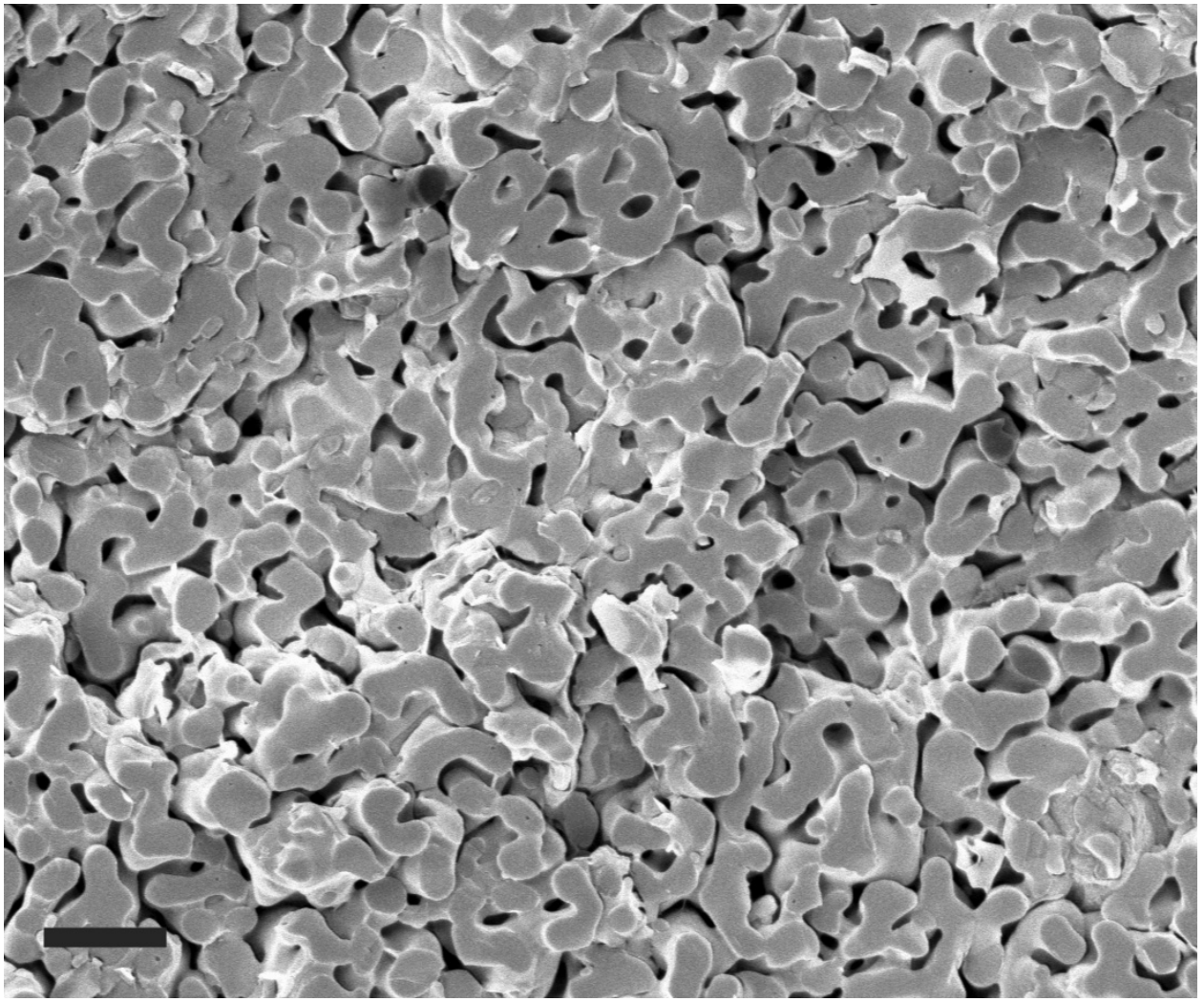

$\alpha = 40$; 34 °C; bar = 1 μm; Davidovich et al., Colloid Polym. Sci. (2015).

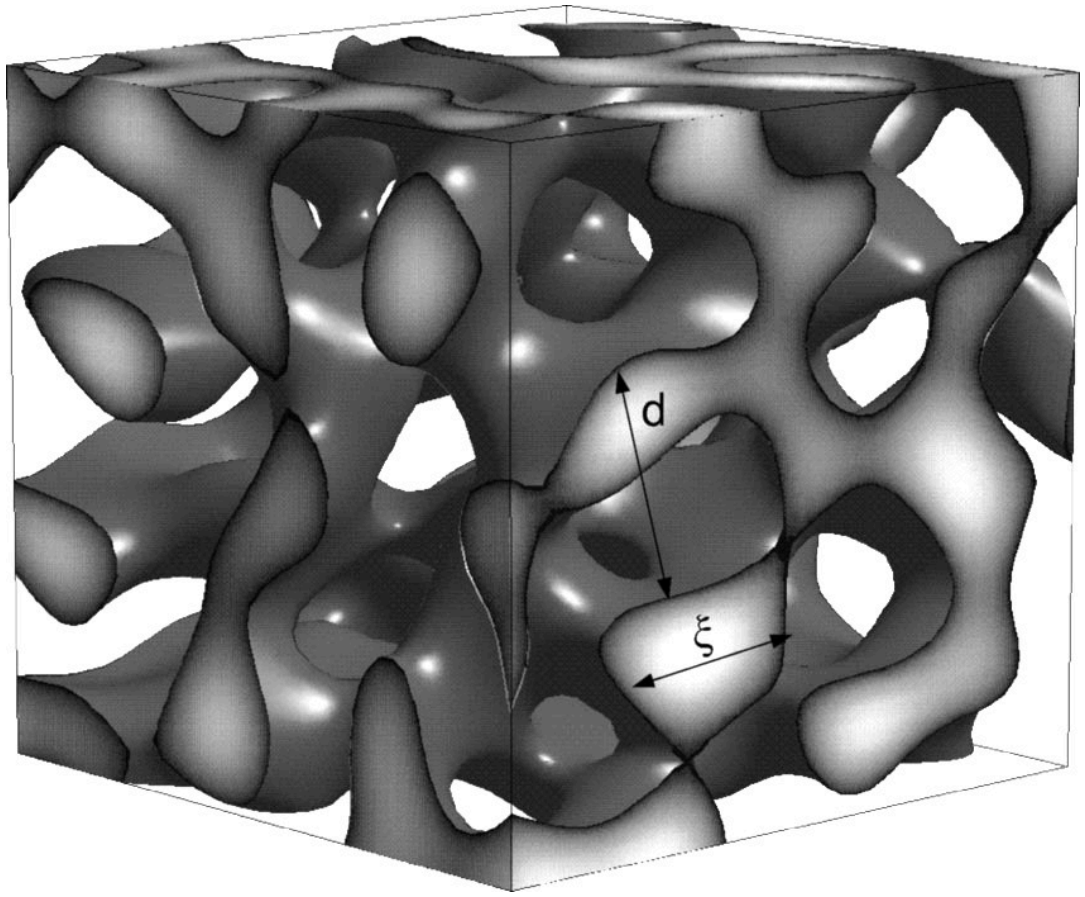

N. F. Berk, Phys. Rev. Lett. 25, 2718 (1987)

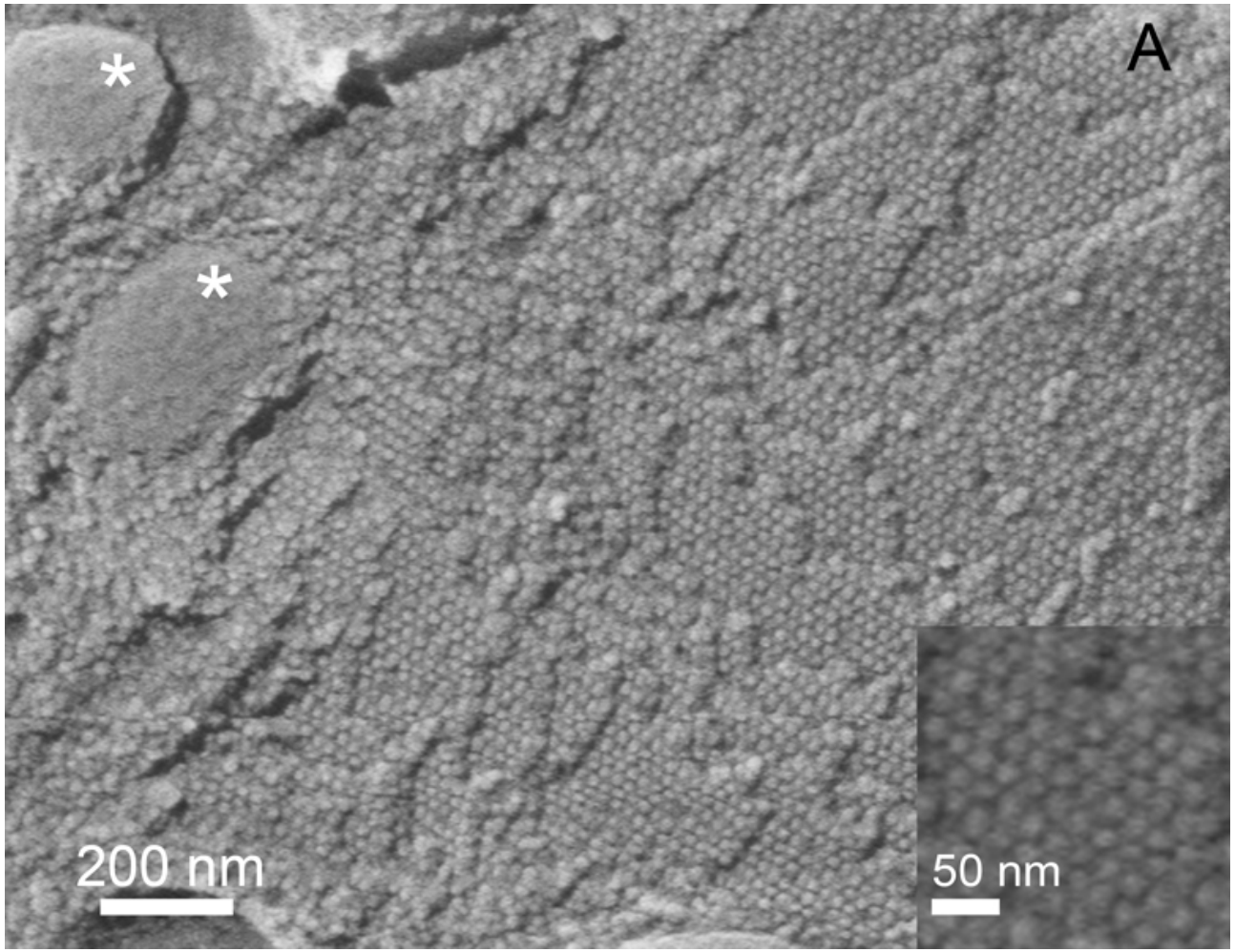

Lecithin/isooctane /water 22/23/55 wt.% *Na'ama Koifman,* J. Phys. Chem. B (2013)

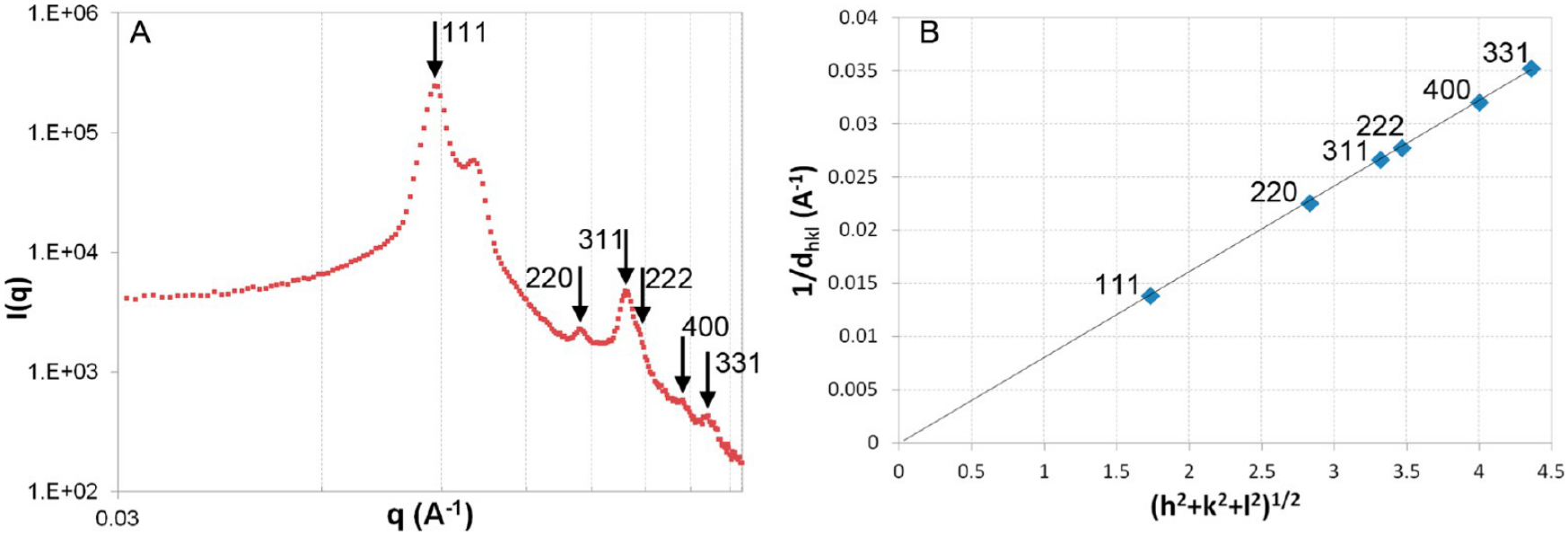

SAXS pattern of 60/32.8/7.2 wt % lecithin, isooctane and water at 25 °C. The arrows mark the positions reflections of the Fd3̄m space-group. The remaining is attributed to a lamellar phase coexisting with the cubic phase in the gel. (B) Plot of the reciprocal d-spacings of the reflections marked in (A).

Lecithin/isooctane /water 22/23/55 wt.% *Na'ama Koifman*, J. Phys. Chem. B (2013)

CNTs Morphology before Dissolution

HR-SEM

AC299P powder

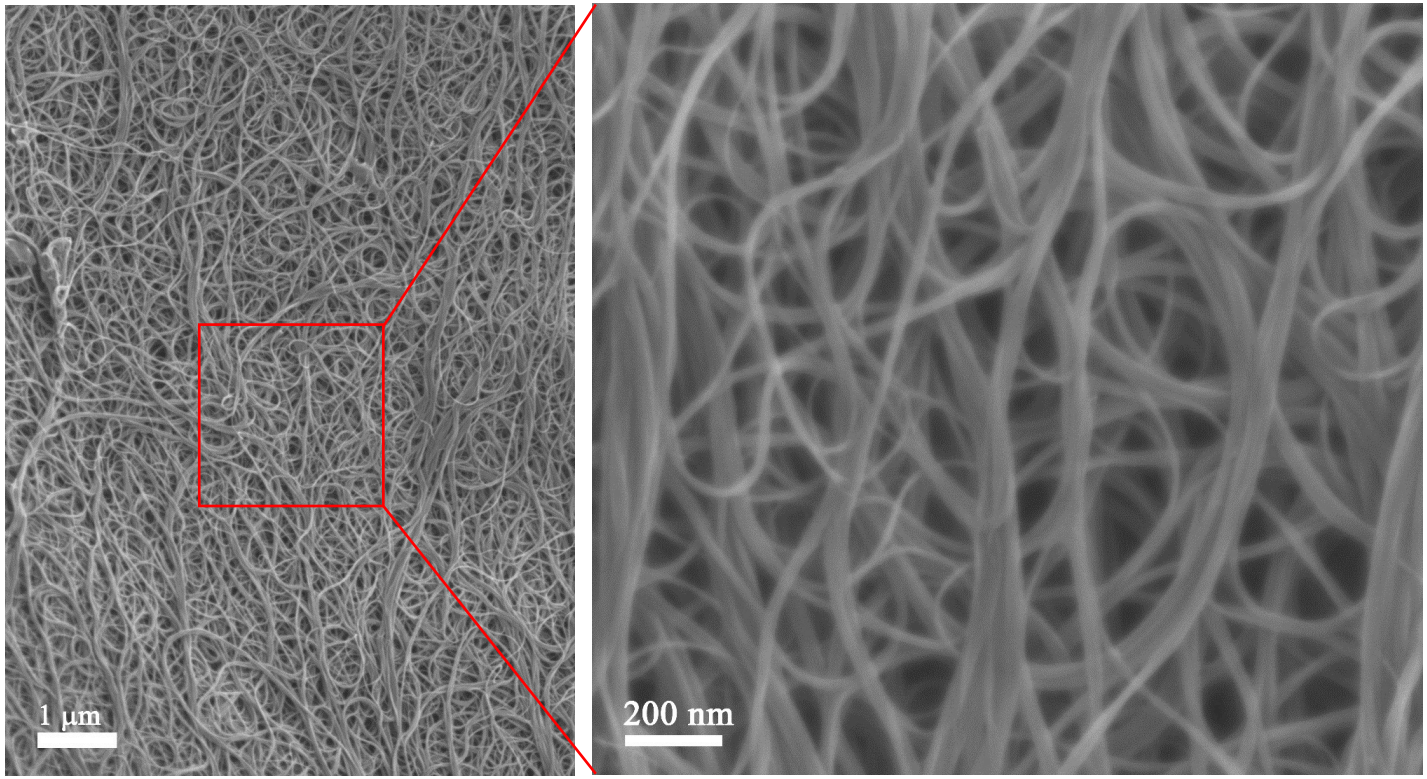

Lucy Liberman

CNTs Solvent of Choice

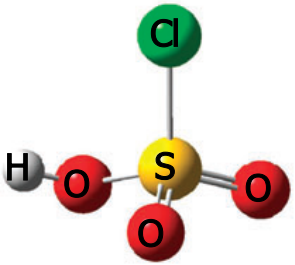

Chlorosulfonic acid (CSA)

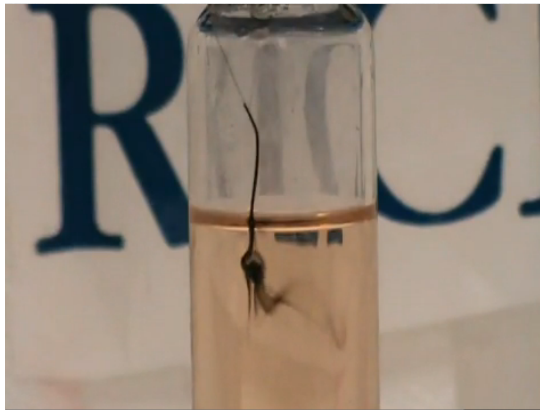

Matteo Pasquali, Rice U

CNT as a rigid-rod polymer

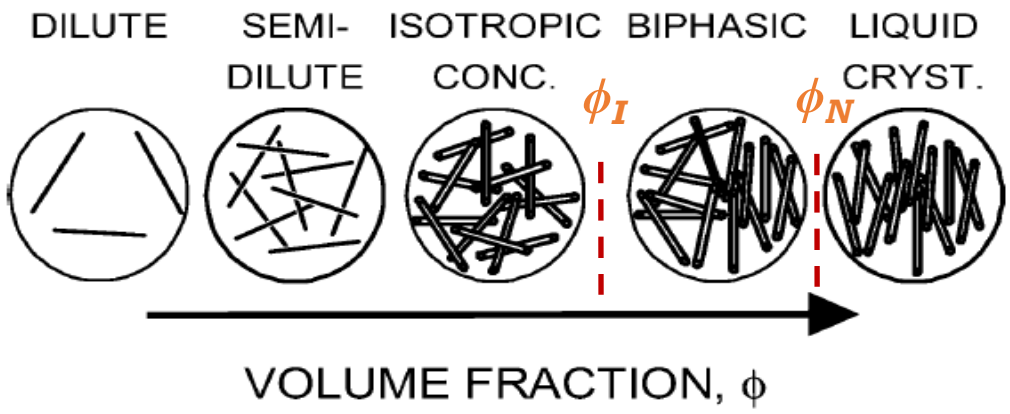

$$\phi_{\mathrm{I}} = 3.29(d/L) \text{ and } \phi_{\mathrm{N}} = 4.19(d/L)$$

ϕ_I and ϕ_N depend on the solvent quality and aspect ratio of the molecules (CNTs)

After Doi, M. and Edwards, S. F.,.
The Theory of Polymer Dynamics; Oxford University Press,1986;
model of Flory, P. J., Proc. R. Soc. London, Ser. A (1956).

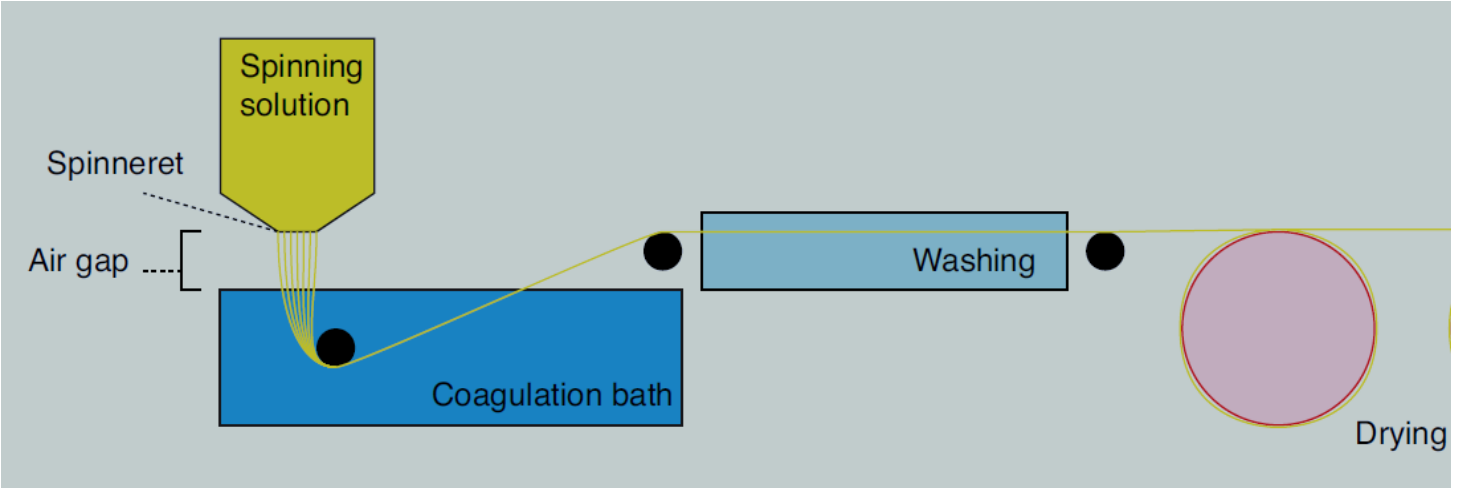

Fiber spinning from nematic liquid crystalline phases of rod-like polymers

20 ppm AC299 CNTs

in chlorosulfonic acid

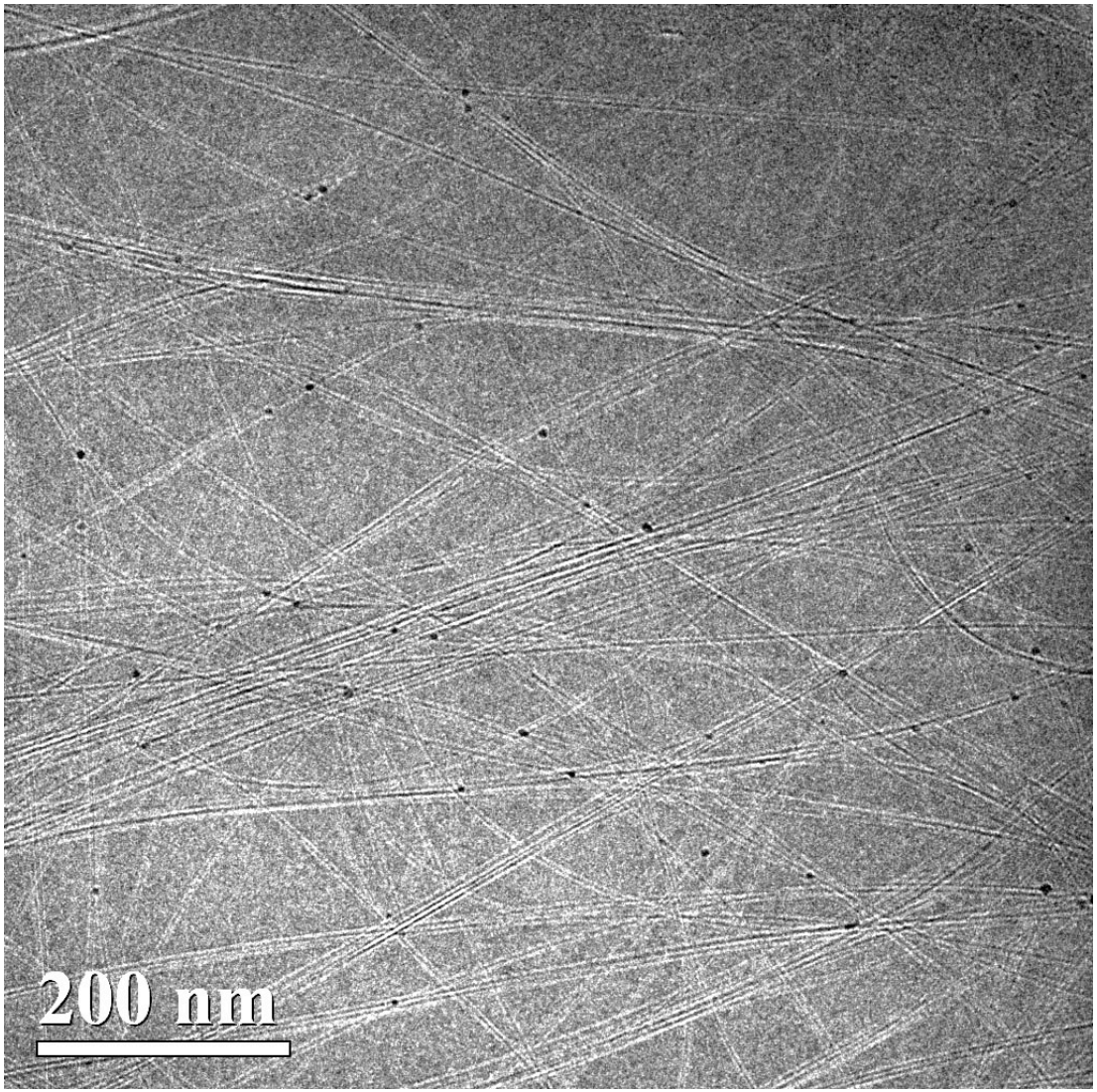

200 ppm AC299 CNTs in

chlorosulfonic acid

Kleinerman, Liberman et al.
J. Microscopy (2017)

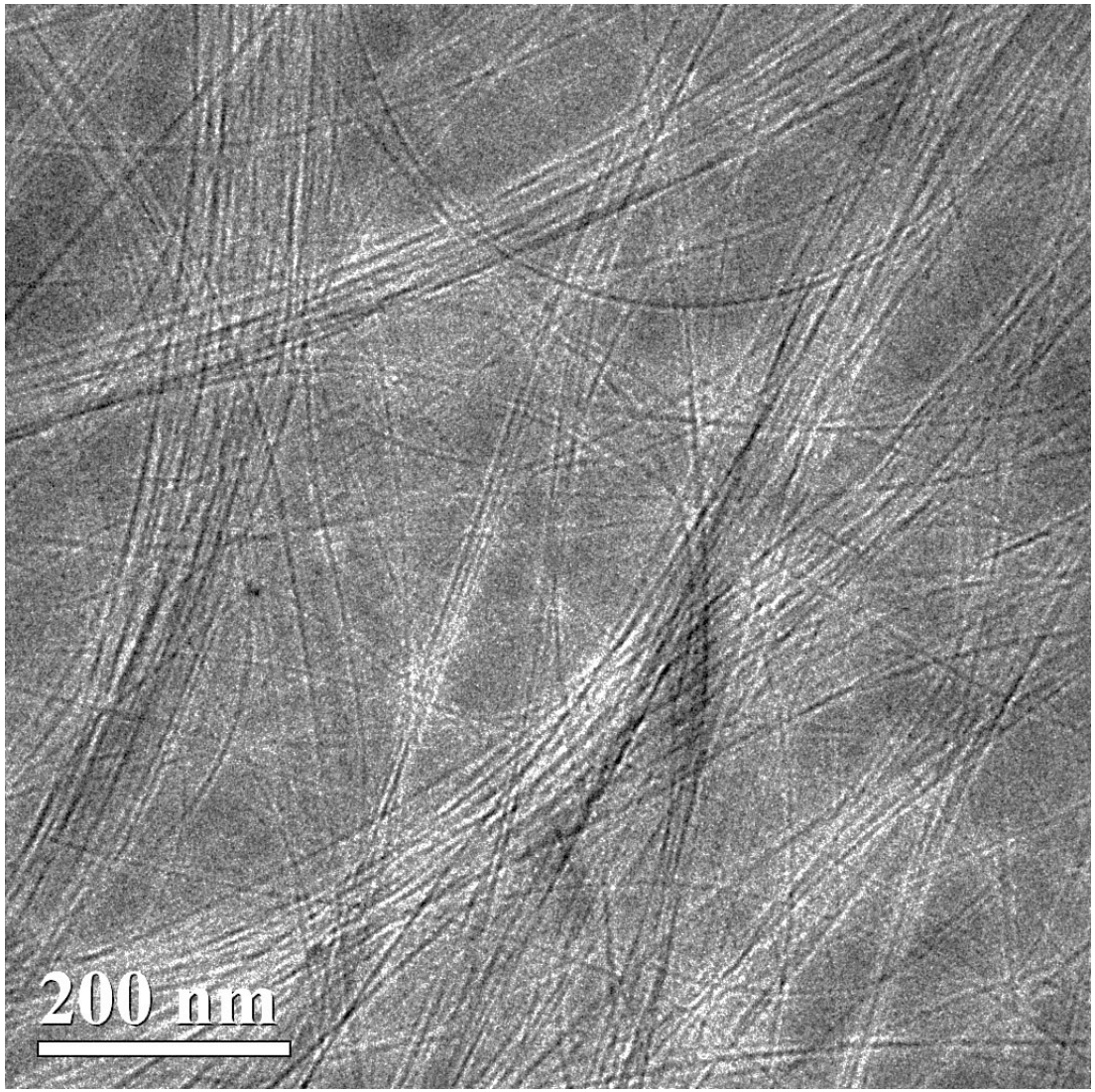

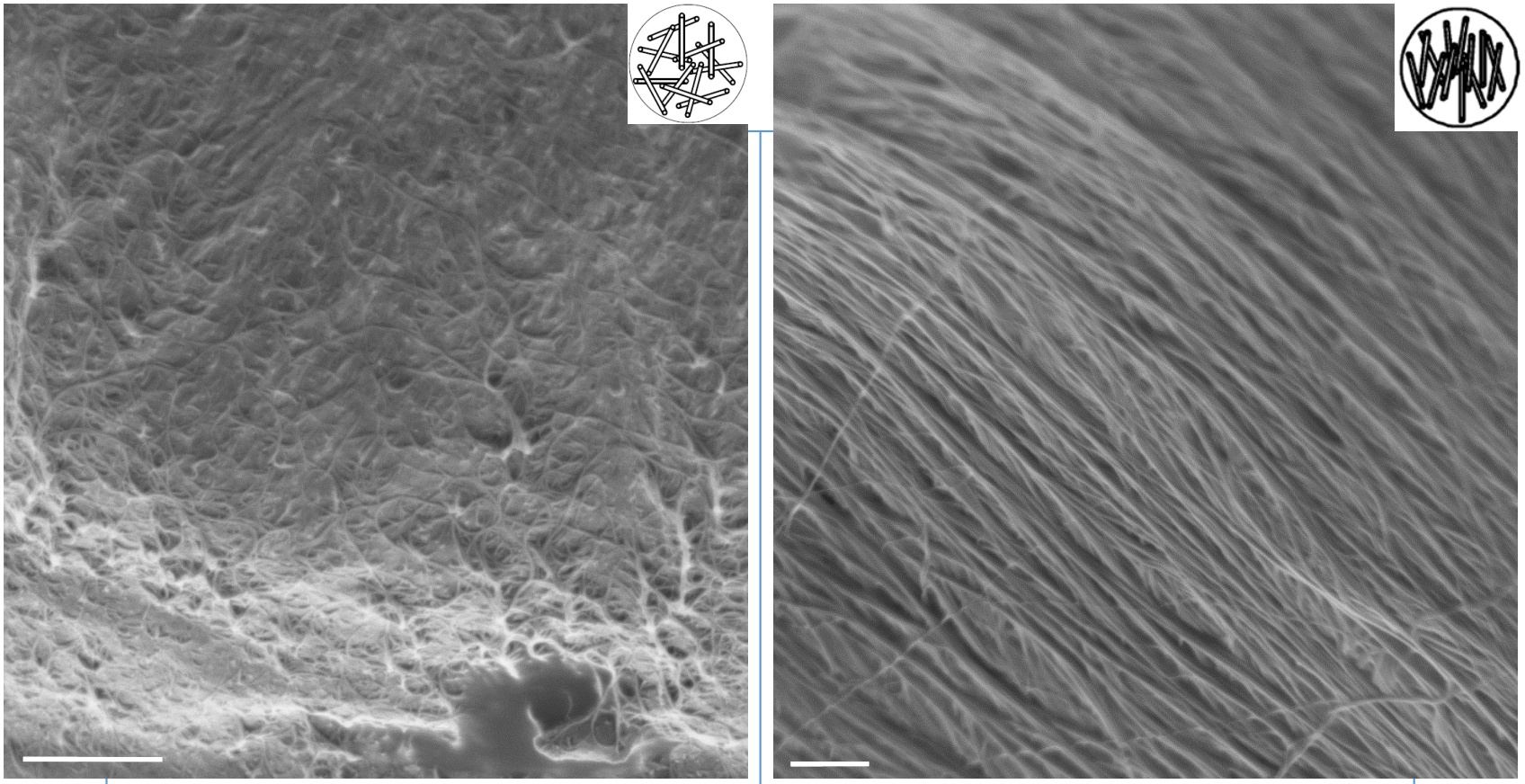

HiPco, 0.7%wt - isotropic phase	CCNI 1101, 3%wt - LC phase

Kleinerman et al., J. Microscopy (2015) ; Matteo Pasquali, Rice Univ.

Bars = 500 nm

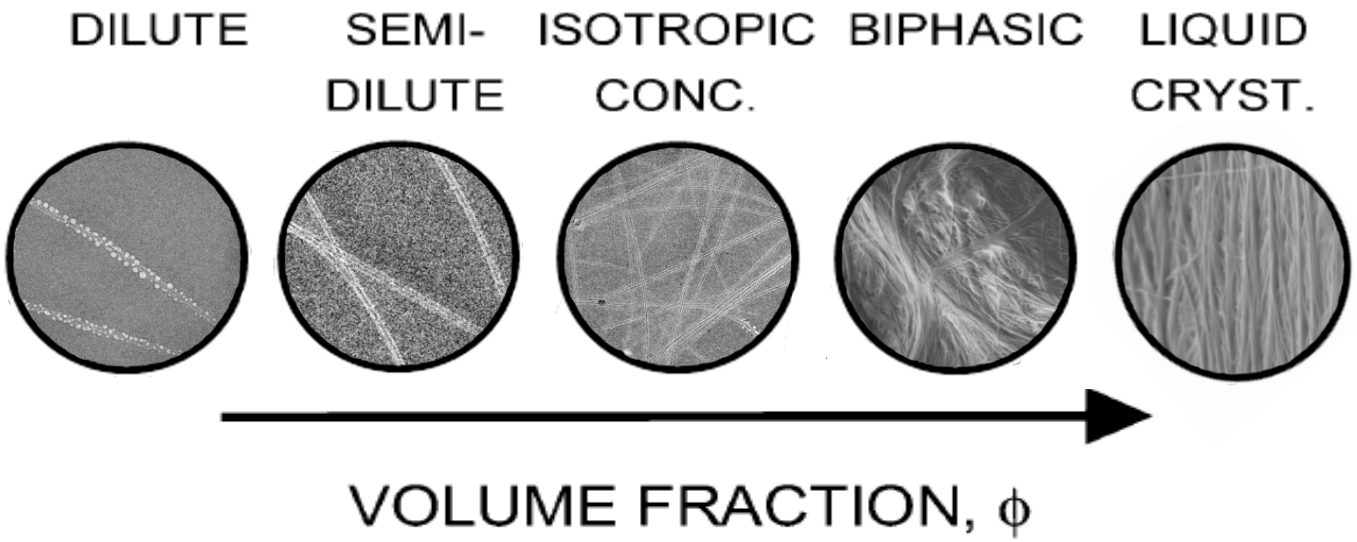

After Doi, M. and Edwards, S. F.,.
The Theory of Polymer Dynamics; Oxford University Press,1986; model of Flory, P. J., Proc. R. Soc. London, Ser. A (1956).

Kleinerman, Liberman et al., Langmuir (2017)